QUARTERLY PROGRESS REPORT

RESEARCH ON PHYSICAL AND CHEMICAL PRINCIPLES AFFECTING HIGH TEMPERATURE MATERIALS FOR ROCKET NOZZLES

December 31, 1964

UNION CARBIDE RESEARCH INSTITUTE
Tarrytown, New York

Project Supervisor Richard W. Kebler
Richard W. Kebler

Submitted by: S. R. Aspinall
S. R. Aspinall, Manager
UC Research Institute

Verner Schomaker
Associate Manager
UC Research Institute

Sponsored by
Advanced Research Projects Agency Propellant Chemistry Office,
ARPA Order No. 34-63, Task 4
Monitored by
Army Missile Command
Contract No. DA-30-069-ORD-2787
Project Code Number PRINCIPIA

FOREWORD

This research program is being carried out in the research laboratories of Union Carbide Corporation located at Tarrytown, New York (Union Carbide Research Institute). The work is supported by the Advanced Research Projects Agency under Contract No. DA-30-069-ORD-2787 with the U. S. Army Missile Command, Redstone Arsenal, Alabama. The report period is from October 1, 1964 to December 31, 1964.

The program at Union Carbide Research Institute is supervised by Dr. Richard Kebler with Dr. S. R. Aspinall serving as general project coordinator and Manager of the Institute.

The scope of the program as stated in the contract is "to obtain a better understanding of the mechanisms which govern the behavior of materials in high-temperature environments, to learn how to make the most effective use of available materials, and to obtain a better knowledge of optimum properties desired for new materials for particular use. The work is expected to provide guidance for those concerned with the development of materials and the use of materials in solid-propellant engines."

TABLE OF CONTENTS

I SUMMARY

An extensive series of measurements of the rate of oxidation of tungsten by CO_2 in the presence of CO was run to explore the validity of the back reaction term in the rate equation

$$r = \frac{AP_{CO_2} e^{-\alpha/RT}}{1 + BP_{CO_2} e^{-\beta/RT}} \left(1 - \frac{P_{CO}\, P_{W_3O_9}^{1/9}}{K\, P_{CO_2}} \right).$$

The values of the constants A, α, B, and β are still provisional.

Experimental rates are compared with those calculated from the above equation and its auxiliary diffusion equations. It is clear that our model predicts the effect of CO very well over the range of conditions studied. Further studies with higher CO/CO_2 ratios are indicated because the reduction in reaction rate found is relatively small.

Samples of Linde swaged, UCCP plated, UCRI arc-melted and General Electric swaged tungsten, the last cut both perpendicular and parallel to the cylinder axis, were oxidized in 100 torr CO_2 flowing at 9000 cm/sec. All reacted at rates that fell on a single log rate vs. 1/T curve. The small degree of scatter in these data reflects the improved control of conditions that has been achieved by modifications of the arc-image apparatus. Since the General Electric tungsten was cut from one of the billets procured for construction of the nozzle inserts to be used in the forthcoming rocket tests the kinetic parameters already derived should be applicable in interpreting these tests.

Enough progress has been made with the tungsten-HF reaction for us to be confident that using the arc-image reactor, we can investigate the kinetics of this reaction over a useful range of temperatures and HF pressures. Much of the equipment needed has already been built and tested. Both the rate of corrosion and the apparent activation energy are much lower for tungsten in HF than for tungsten in CO_2 under our conditions of pressure, temperature, and flow.

Work on the analysis of stagnation-flow reactors has continued. The procedure chosen for the numerical solution of the stagnation-line equations consists of reduction of these equations to a set of first-order equations,

forward integration from estimated initial (surface) conditions, and refinement of the initial conditions to yield desired end-point values. We are now able to integrate stagnation-line equations for constant composition, viscosity, thermal conductivity and heat capacity. The restriction of constant composition will next be removed by introducing the equations of continuity of species and the diffusion equations.

A test motor (1FRNA-UIMH) for nozzle-insert corrosion testing is being designed by the Army Missile Command to operate with constant fuel and oxidizer feed rates at chamber pressures up to 1000 psi. Estimates of the nozzle-insert heating show that to reach the desired operating temperatures the tungster insert must be thermally insulated from its holder. A proposed nozzle-insert and holder design was submitted to the Propulsion Laboratory for mating with the motor aft closure. The measurements and associated calculations to be made are discussed.

A plausible kinetic model for the oxidation of tungsten has been deduced from our earlier mass-spectrometric measurements. The various rate constants so established may be used to estimate the rate of the oxygen-tungsten reaction at temperatures and pressures such that the surface conditions are similar to those that prevailed during the experiments. The present method of prediction yields agrees with the experimental results of Perkins et. al. to ca. 50% at 2000°K and 0.1 to 3 torr O_2; at higher and lower temperatures the agreement is not as good, but still commendable.

Vapor species formed by the reaction of molecular oxygen with molybdenum were identified and the ion intensities measured as a function of surface temperature and oxygen pressure over the ranges 1472° to 2437°K and 10^{-6} to 2×10^{-4} torr O_2. The principal products are $MoO_3(g)$, $MoO_2(g)$, $MoO(g)$, and $O_2(g)$.

The high-temperature furnace for the Siemens diffractometer, operated with a helium atmosphere to minimize surface boron loss, was used to collect x-ray diffraction data for MnB_2 up to 1114°C, from which lattice constants (still tentative) were calculated by least-squares. Mass-spectrometer studies show that the losses of boron experienced for MnB_2 at about 1000°C in vacuum may be by way of reaction with traces of water to form $(HBO)_3$. Lattice constant and thermal expansion data obtained for a new sample of TiB_2 up to 2041°C agree excellently with the data obtained earlier from a different sample by a different technique.

agreement between lattice constants before and after the 2041°C run indicates that little boron was lost.

Measurements of the elastic moduli (C_{11}, C_{12}, and C_{44}) of single-crystal tungsten as functions of temperature to 1800°C have been completed. A report on this work is being prepared. No further work on dynamic elastic properties is planned except as needed for studies of composite materials.

High-temperature creep has been followed as a function of stress at constant temperatures for three more large-grained polycrystalline TiC specimens. Two of these were presumably much purer than previous specimens and their creep rates were much larger. The less pure specimen showed a high stress dependence ($\sim\sigma^{10}$) comparable to the stress dependence reported for an earlier specimen of equivalent purity. The two purer specimens showed the smaller stress dependencies $\sigma^{6.0}$ and $\sigma^{6.2}$. The plastic deformation of TiC is a very sensitive function of structure and impurities, which suggests that the high-temperature mechanical properties of TiC specimens in general will also be highly dependent on their thermal and mechanical history.

Satisfactory zone melting of 1/4-inch tungsten rod is anticipated with equipment on order for the automatic control of bombardment current in the electron beam zone refiner. Since single-crystal specimens of tungsten cannot yet be made here, initial measurements of steady-state creep are to be made on single-crystal specimens of Mo obtained from Union Carbide European Research Associates.

Very good results have been achieved in the electrolytic machining of 1/4-inch tungsten rod. A tensile specimen 4-inches long with a central 5/8-inch gauge section and 1/4-inch long cylindrical knobs on each end has been produced.

The pyrohydrolytic determination of boron in zirconium diboride and titanium diboride was successfully applied to the diborides of tantalum and niobium, and, with some modifications, to hafnium diboride as well. The results are in general agreement with the results obtained by use of the routine peroxide fusion method but indicate better boron recovery by pyrohydrolysis than by the peroxide fusion.

Skeletal carbide composites are designed to be superior in low-temperature [illegible] for the refractory carbide itself, while maintaining its

desirable high-temperature properties even though the metal may melt or vaporize. Such behavior, as measured by transverse rupture strength, has now been found for TaC-Ag composites. One check on the probable behavior of an infiltrated composite at elevated temperatures is to determine the properties of the skeleton after complete vaporization of the infiltrant. Silver-infiltrated TaC specimens so treated had substantially the same strength, density, and resistivity as the original hot-pressed TaC. The attractive feature of the Ag-TaC composite is that it is generally stronger than the original TaC from room temperature to about 1400°C and comparably strong at 1800°C. The infiltration and the subsequent vaporization of the silver apparently do not disrupt the TaC grain-to-grain bonds.

The transverse rupture strength of the TaC-Ni composites is high at room temperature but drops drastically at 1400°C. Furthermore, when the TaC-Ni composite is heated to high temperatures (over 2000°C) to drive off the nickel, the carbide skeleton remaining is porous and friable and easily broken by hand. The carbide-carbide bonds are evidently disrupted by the nickel at temperatures at and above its melting point. Methods that may minimize this disruption are being studied.

Hot-pressed ZrC bars (80-90% of theoretical density) made from purified ZrC powders have been infiltrated with nickel or with silver, but with irregular results. Sometimes the specimen infiltrated completely, but sometimes only a shallow surface layer seemed to be affected. Further work on ZrC-based composites is desirable because they may well have better resistance to high-temperature corrosion than TaC and NbC composites have.

An additional means of achieving skeletal strength at very high temperatures, and also of making use of any possible advantage derived from the Group IV carbides, is the use of carbide solid solutions. Batches of 80 TaC/20 HfC, 90 TaC/10 HfC, 80 TaC/20 ZrC, and 90 TaC/10 ZrC have been prepared and used to make both transverse rupture strength specimens and infiltration blanks. In preliminary infiltration experiments these compositions behaved similarly to TaC, indicating that essentially continuous fine porosity can be achieved reproducibly for these solid solution carbides.

II INTRODUCTION

This program is concerned with the principles governing high-temperature chemical and physical behavior, especially in the respects that may contribute importantly to the successful performance of materials as rocket components operating at high temperatures.

The materials being studied here are tungsten, graphite, and the refractory carbides and borides of the transition metals. These carbides and borides are difficult to handle because of their high melting points, brittleness and high hardness at room temperature, and susceptibility to contamination at high temperatures. Thus, a considerable effort is devoted to their purification and fabrication. Composite bodies consisting of interpenetrating carbide and metal skeletons are being prepared and evaluated. These appear to hold promise for high-temperature service, especially in rocket nozzles.

Because corrosion of rocket nozzles by the exhaust gases is a serious problem, reaction rates between various gases or combinations of gases and possible nozzle materials are being studied as functions of temperature and pressure in this program. However, at typical temperatures for rocket operation these gas-solid reactions may be controlled not by the surface reaction rate but partly or entirely by the rates of diffusion of reactants to the surface or of products away from it. Special efforts are being made to measure truly surface-controlled reaction rates for the various refractory materials at all temperatures of interest by using experimental conditions that afford very high mass-transfer rates. The values so obtained will permit calculation of corrosion rates for conditions where both surface reaction rate and diffusion are important.

As structural parts, rocket nozzles are subjected to substantial stresses during operation. Some of these stresses change relatively slowly with time, and their effects on the nozzle will be determined by creep strength and ductility. There are also rapidly changing stresses, resulting from sudden heating or cooling, which can cause deformation or fracture. The thermal stress developed by a given temperature change increases with increasing coefficient of expansion or elastic modulus, and decreases with increasing thermal conductivity or specific heat, and the likelihood of fracture due to these stresses further depends upon the tensile strength and ductility. Measurements are being made of several of these important properties.

III. TECHNICAL RESULTS AND PLANS

A. Gas-Solid Reactions

Introduction

In the September 1963 Quarterly Progress Report (QPR) the relationship between gas-phase diffusion and surface kinetics of gas-solid reactions was discussed in some detail. There and in the following QPR (December 1963), it was pointed out that many important corrosive reactions are sometimes controlled by gas diffusion and sometimes by surface kinetics, depending on the conditions of temperature, pressure, and flow. If the effect of a corrosive environment on a refractory material is to be predicted, therefore, rate expressions for the potential reactions must be available from laboratory studies approaching as closely as possible the conditions of temperature and pressure of that environment. However, slowness of gas-phase diffusion can interfere with laboratory measurements just as it affects the practical situations. Each experiment intended to provide surface-kinetic data must therefore be carefully analyzed with respect to gas diffusion and designed to minimize its effects.

Our first objective is the determination of the surface-controlled rates of reactions between gaseous rocket exhaust components and actual or potential rocket nozzle materials in the range of temperatures and pressures characteristic of rocket operations. Our second objective is the development of methods of applying such rate data, in conjunction with aerodynamic analyses, to predict corrosion rates in the transition region between surface and diffusion control. To weigh the extent of control by gaseous diffusion all the data obtained in this program are being analyzed to determine where diffusional effects are important.

We have designed and built a number of experimental reactors in which high mass-transfer rates are achieved through use of high velocity gas streams impinging in stagnation patterns on hot samples; the effect for a given reaction is to raise very considerably the temperatures at which gaseous diffusion becomes important in determining observed reaction rates, thus allowing the measurement of purely surface-controlled reaction rates to be made

at higher temperatures than otherwise possible. Section A-3 continues the development of the theory of mass transfer in such systems.

A study of the effect of CO on the kinetics of the oxidation of tungsten by CO_2 in our sub-atmospheric stagnation-flow reactor is described in Section A-1. Further investigations of the effect of tungsten preparation on the kinetics of this same reaction are reported in this section also. Progress in our study of the kinetics of the HF-W reaction is described in Section A-2.

The experimental arrangements described above, though capable of yielding rate expressions at temperatures and pressures of direct interest in rocket propulsion, all operate under conditions that preclude observation of the details of the gas-surface reaction mechanisms. To obtain this type of information mass-spectrometric studies of reactions at very low pressures are being conducted; the results obtained by this technique for the O_2-W and O_2-Mo reactions are discussed in Section A-5.

We plan to test the applicability of our models for predicting corrosion rates by comparing predicted with actual nozzle insert corrosion rates. The status of this program is discussed in Section A-4.

1. Kinetics of the Oxidation of W by CO_2 — R. A. Graff, I. R. Ladd, J. M. Quets, P. N. Walsh

The induction-heated stagnation-flow reactor being used to measure rates of corrosion of tungsten by carbon dioxide at pressures below one atmosphere has been described (QPR March, June 1964). Briefly, the experiments involve flowing a metered mixture of Ar and CO_2 at room temperature in a stream perpendicular to one face of a cylindrical tungsten sample heated by a current concentrator. The total pressure of the reacting mixture is the stagnation pressure over the tungsten surface and the temperature of the reacting surface is measured by an optical pyrometer during the course of the experiment. The rate of surface recession at the stagnation point is the desired reaction rate; it is ordinarily multiplied by the ratio of the density of tungsten to its atomic weight to obtain the rate in moles/cm^2 sec.

In the September 1964 QPR, details of the analysis of our data on the kinetics of the oxidation of W by CO_2 were presented; the choice of rate equation 1)

$$r = \frac{AP_{CO_2} e^{-\alpha/RT}}{1 + BP_{CO_2} e^{-\beta/RT}} \left(1 - \frac{P_{CO}\, P_{W_3O_9}^{1/9}}{K\, P_{CO_2}} \right) \qquad (1)$$

and the determination of the constants A, α, B, and β in this equation by a least-squares technique were discussed. At that time, the iterative least-squares calculation had not converged though a reasonable fit to the data had been obtained. The calculation has now been carried to convergence; the agreement between observed and calculated rates can be seen in Figure A-1, which includes all the points involved in the calculation. This figure can be compared with Figures A-8, 9, and 10 of the September 1964 QPR, which show the previous fit. The values of the constants* at convergence are

$A = 15{,}648$ moles/cm^2 sec. atm
$\alpha = 90{,}891$ cal/mole
$B = 1.657 \times 10^{-5}$/atm
$\beta = -55{,}234$ cal/mole.

---

* The fifth parameter, Nu', which is involved in the diffusion equations that are solved simultaneously with the rate equation (cf. QPR September 1964) now has the value 237.0.

These constants are still to be regarded as provisional, because (v.i.) the temperature uncertainties discussed in the September 1964 QPR have not been entirely cleared up.

Extensive measurements of the rate of oxidation of tungsten by CO_2 in the presence of CO were made to explore the validity of the back reaction term in the rate equation (1). In one set of runs, the CO/CO_2 ratio was varied while the flow of Ar was kept constant at 54 SLM and the total flow of CO_2 + CO at 30 SLM. In the two other sets, the CO_2 and CO pressures were varied, while the CO/CO_2 ratio was held constant. The experimental rates are compared in Figures A-2, A-3, and A-4* with those calculated from our model (Equation (1) and its auxiliary diffusion equations) with the parameter values listed above. It is clear that the model, which was deduced in the absence of any experimental data from CO runs, satisfactorily predicts the effect of CO observed so far. However, further studies with higher CO/CO_2 ratios seem indicated because the reduction in reaction rate found is relatively small – its maximum extent is shown in Figure A-5 where the observed rates at 20 torr CO_2 and 101 torr CO (in 219 torr Ar) are compared with those calculated from the model for these conditions and for 20 torr CO_2 in 320 torr Ar. In this case, the CO effect is seen to be somewhat over-predicted. It can be concluded, however, that the form of back-reaction term employed is reasonable and that CO has no appreciable effect on the forward rate.

In the arc-image reactor, samples of Linde swaged, UCCP plated, UCRI arc-melted, and General Electric swaged tungsten, the last cut both perpendicular and parallel to the cylinder axis, were oxidized in 108 torr CO_2 flowing at 9700 cm/sec. All reacted at rates that fell on a single log-rate vs. 1/T curve (Figure A-6). The notably small scatter reflects improved experimental control, achieved by modifications of the arc-image apparatus, as described below and in previous reports. Also shown in Fig. A-6 are the rates predicted by our model, using again the parameter values derived solely from data obtained in the induction-heated reactor on Fansteel tungsten. The curves differ by roughly a factor of two in rate or 80° in temperature; this is not bad in view of the differences in experimental techniques, but the discrepancy is large enough to have prompted us to undertake a thorough recalibration of our

---

* Some of the data in Figure A-2 were presented in Figure A-11 of the September 1964 QPR.

methods of measuring temperature and flow. Since the General Electric tungsten was cut from one of the billets procured for construction of the nozzle inserts to be used in the forthcoming rocket tests (cf Sec. A-4) it seems that the kinetic parameters already derived should be adequate for interpreting these tests.

The copper inlet tube (Figure A-7) with improved purge-gas exit tube that was developed for HF work differs from its predecessor in that the protective sheath of argon does not dissipate its momentum as rapidly as before; consequently, the reaction products are swept away more efficiently and the reactor walls stay clean longer. This tube has performed very well for the CO_2-W reaction, also.

A larger and optically better external mirror has been installed in the arc-image furnace. It is now possible to heat samples to at least 2900°K in a glass reactor and to melt thoria (3350°K) in the open.

Temperature Corrections - In the June and September 1964 QPR's it was reported that samples used in the stagnation-flow reactors show different degrees of gross surface roughness after reaction, this being greater when the reaction occurs under conditions approximating surface-rate control than when gaseous diffusion is important. Such differences in sample surface conditions can cause the emittance, and hence the correction from brightness temperature to true temperature, to be different for different samples.

An unsuccessful attempt was made to determine the reflectivities, and hence the emittances, of a representative group of reacted samples from the induction-heated stagnation-flow reactor by directing a beam of 0.65μ light nearly normal to the surface and focusing the light reflected in all directions onto a photocell. A sample of powdered MgO (reflectivity assumed unity) was used as a reference. No way was found to ensure that only the reacted part of the sample was illuminated, and the measurements scattered excessively. Since the more direct emissivity measurements described below and in Section A-3 of the September 1964 QPR indicate that the room-temperature and high-temperature emissivities may not be the same for these samples, high-temperature measurements will be carried out on samples from the induction-heated reactor.

Half of the oxidized surface of each of four Linde samples and six G. E. samples studied in the arc-image reactor was carefully repolished after reaction, then reheated in pure argon to 2600°K to 2700°K. In none of the ten samples was there any discernable difference in brightness temperature between the polished half and the oxidized half. Since there is no reason to suppose that the two sides of the sample were at appreciably different temperatures and since a test with a piece with half the face sandblasted indicated that brightness temperature differences of ten degrees between adjacent surfaces are very easily discerned, it is concluded that the oxidized surfaces differed by no more than 0.01 in emittance from the polished surfaces, even though to the unaided eye the reflectivity and consequently the emittance seemed to have changed considerably. Microscopic examination (Figure A-8) of the oxidized samples showed that each surface was made up of small, highly reflective, non-parallel areas of transverse dimensions generally much larger than 0.65μ, the wavelength of light utilized by the pyrometer. On the other hand, the reflecting areas of the sandblasted sample (Figures A-8a,c) and the oxidized low-density Rembar tungsten (reported on last quarter) were very small, probably approaching 0.65μ. Thus far, only the low-density Rembar material has required emittance corrections other than standard literature values.

Hyper-Baric Stagnation-Flow Reactor - During this quarter, several measurements of the rate of reaction of tungsten with CO_2 at a velocity of 1.34×10^4 cm/sec were made; these showed a very poor reproducibility because the experimental difficulties with temperature control could not be overcome. As explained in the September 1964 QPR, when CO_2 impinges on the tungsten surface the temperature is substantially lowered and this lowering continues during the course of the experiment. The solution now under study is to increase the power input fast enough to keep the temperature constant; if this method gives good results, an automatic temperature control will be installed.

Water-Vapor Studies - Equipment for using water vapor as the reactive component in the gas is being assembled and tested. Experimental difficulties still exist. A critical-flow nozzle for metering the water vapor is now being calibrated.

2. The W-HF Reaction R. A. Graff, I. R. Ladd, P. N. Walsh

Enough progress has been made with the tungsten-HF reaction for us to be confident that we can investigate the kinetics of this reaction over a useful range of temperatures and HF pressures. Already built and tested are (1) a leak-free system for handling gaseous hydrogen fluoride impinging upon the sample face at velocities up to 9000 cm/sec, (2) cam-operated HF valves with relatively large orifices, and (3) a nozzle system (also used for the tungsten-CO_2 reaction, see Figure A-7) providing a flow pattern such that a glass reactor can be used without becoming fogged during a run.

The significant data obtained thus far are shown in Figure A-9 and compared to corrosion by an equivalent partial pressure of CO_2 in Figure A-6. In three other runs the temperature varied by 100 to 200 degrees for reasons not yet understood. Twice, however, it has been possible to hold the temperature within a range of ten degrees for periods of five minutes.

Both the rate of corrosion and the apparent activation energy are lower for tungsten in HF than for tungsten in CO_2 under our conditions of pressure, temperature, and flow.

We hope next quarter to accomplish a fairly extensive study of the tungsten-HF reaction.

3. Analysis of Stagnation-Flow Reactors R. A. Graff, P. N. Walsh

The procedure chosen for the numerical solution of the stagnation-line equations (QPR June 1964, p. III-30ff) consists of reduction of these equations to a set of first-order equations, forward integration from estimated initial (surface) conditions, and refinement of the initial conditions to yield desired end-point values. This procedure was chosen because computer library routines were available for the forward integration and the refinement of initial conditions.

Instabilities in the forward integration were noted in the September 1964 QPR. Because of the complexity of the problem, it was not possible to discover the cause of the instability by working with the full set of equations. Consequently, we have taken the approach of starting with a simple version of the problem (flow at constant pressure, temperature, and composition) and adding complexities one at a time. In this way we have progressively removed the restrictions of constant pressure and of constant temperature.

Several points have so far emerged. First, successful forward integration requires careful selection of initial conditions. Poor initial conditions have been found to result in a divergence of the integration. Proper values have been found by trial. Second, the integration must be carried to more than one-third the distance to the nozzle before velocity and temperature (composition has not yet been explored) reach values appropriate to the external solution. With proper initial conditions, integration to the nozzle exit is performed without difficulty and with little additional computation time. We now do this and so avoid the complexities associated with the use of the external solution.

It has been found necessary to modify the z-momentum equation (QPR June 1964, p. III-39, Eq. 4). The case of constant temperature and composition may be used to illustrate the difficulty. For this case, with the use of the continuity equation, the z-momentum equation becomes

$$\frac{\rho v_z}{g_c}\frac{\partial v_z}{\partial z} + \frac{\partial P}{\partial z} = -\mu\left[2\frac{\partial w}{\partial z} + \frac{4}{3}\frac{\partial}{\partial z}\left(v_z\frac{\partial \ell n \rho}{\partial z}\right)\right] \qquad (1)$$

Since ρ is directly proportional to pressure under the conditions assumed, this is a second order equation in pressure,

$$\frac{\partial^2 \ell n P}{\partial z^2} = -\frac{1}{v_z}\left[\frac{3}{4}\frac{P}{\mu} + \frac{\partial v_z}{\partial z}\right]\frac{\partial \ell n P}{\partial z} - \frac{3}{2}\frac{1}{v_z}\frac{\partial w}{\partial z} - \frac{3}{4}\frac{\rho}{\mu g_c}\frac{\partial v_z}{\partial z}, \qquad (2)$$

which has a singularity when v_z is zero. However, v_z is zero at the origin when there is no reaction and is zero at some interior point when corrosion occurs. To remove this singularity we have assumed that compressibility has a negligible effect on the shear rate (i.e. the density term on the right side of Eq. (1) has been dropped) and obtained the first order pressure equation

$$\frac{\partial \ell n P}{\partial z} = \frac{-2\mu\frac{\partial w}{\partial z} + 2w\frac{\rho v_z}{g_c}}{P - \frac{\rho v_z^2}{g_c}}. \qquad (3)$$

No difficulty has been encountered in the integration with this modification.

With the modified z-momentum equation we are able to integrate stagnation-line equations for constant composition, viscosity, thermal conductivity and heat capacity. The restriction of constant composition will next be removed by introducing the equations of continuity of species and the diffusion equations.

A test of the nonlinear estimation library routine (NLE) that is used for adjusting of initial conditions t yield the proper final (nozzle exit) values of the variables has been made for the case of constant temperature, pressure, and composition. With initial guesses for the parameters good enough to yield a successful forward integration, convergence on desired end-point values was obtained without difficulty. NLE will now be used on the more complex problems.

4. Rocket-Nozzle-Insert Test and Analysis Program D. Pugh, P. N. Walsh

A visit was made on November 30, 1964 to the Propulsion Laboratory, Directorate of Research and Development, Army Missile Command to discuss liquid motor firings for corrosion studies on tungsten nozzle inserts. The procedure for calculating the expected corrosion and the experimental information we need from the firings were discussed.

The scheme devised for calculating the rate of corrosion of a test nozzle-insert requires that the mass-flow rate be constant and that the surface temperature be independently known from experimental measurements, as a function of time. A standard flame-temperature and composition calculation for the chosen fuel-oxidizer mixture at the given initial throat pressure will then be used to compute the initial free-stream gas composition. Next, the initial rate of removal of tungsten will be obtained by an iterative solution of the surface rate equations coupled with the film-model diffusion equations (cf. September 1964 QPR, pp IV-6,7). For this part of the calculation, the state of our knowledge requires that we assume as corrosive only those gases for which the rate of removal of tungsten is known as a function of temperature and partial pressure. All others will initially be considered inert; relaxation of this restriction to permit some gas-phase reaction near the surface will be considered later. The mass-transfer coefficient needed in the diffusion equations will be derived from a modified Bartz[1] correlation using an average of the

1. D. R. Bartz, Jet. Propulsion, p. 49 (1957).

free-stream and surface temperatures. The calculated corrosion rate will be considered to be constant for such a length of time as the experimental surface temperature is known to be constant within some preset number of degrees or until the throat cross-sectional area has been calculated to increase by a preset percentage. From the calculated throat area at the end of this period, the new throat pressure will be determined, a new free-stream temperature and composition calculated, and the corrosion calculation recycled. This procedure involves a stepwise summation of the total corrosion, but may be made close to a true integration by choosing small increments of time.

Preliminary calculations show that to reach the desired operating temperatures the tungsten nozzle insert must be thermally insulated from its holder. A proposed insert and holder design has been submitted to Mr. Donald Dahlene of the Propulsion Laboratory.

The test motor (IFRNA-UDMH) is to operate with constant known fuel and oxidizer feed rates at chamber pressures up to 1000 psi. Pressures as a function of time can be determined to ± 1/2% at 1000 psi. Running times up to 60 seconds are possible, and steady combustion conditions in the chamber should be reached in about 100 milliseconds after start.

Determination of the insert interior surface temperature is the principal experimental problem. Present plans are to do this with multiple thermocouple probes in the nozzle insert and also by designing the insert and holder so that a narrow-angle recording pyrometer can be sighted on the insert throat. Because of our uncertain knowledge of emittances the last method will be uncertain; still, it will serve as a check on the thermocouples.

5. Mass-Spectrometric Studies — O. Conrad Trulson, Paul Schissel

a. Tungsten-Oxygen System

The measurements of the pressure and temperature dependence of the oxidation of tungsten have been completed and reported in detail in Technical Report C-26.[1] A plausible kinetic model was deduced and the various rate constants evaluated. The model and rate constants may be used to estimate the kinetics of the oxygen-tungsten reaction under conditions not directly amenable to mass-spectrometric measurement, provided the temperature and pressure are such that the surface conditions are similar to those that prevailed during the experiments.* In terms of the model, the procedure for determining whether the surface conditions are similar rests merely on determining the amount of oxygen adsorbed on the surface. The oxygen is adsorbed on two kinds of sites and the fractional coverage of these sites may be computed as follows. Given the tungsten surface temperature (T, °K) and the oxygen pressure (P, torr), parameter values α and β are computed from

$$\alpha = \frac{1}{P}\, 10^{7.845-3.147(\frac{10^4}{T})} \qquad (1)$$

$$\beta = \frac{1}{P}\, 10^{8.146-1.94(\frac{10^4}{T})} \qquad (2)$$

and these values are used with Figure A-10 to determine $\theta_1(\alpha)$ and $\frac{\theta_2}{\theta_1}(\beta)$. The loss R of tungsten (as WO_2 and WO_3) is then determined from

$$R = k\theta_1^{\,3} \left(\frac{\theta_2}{\theta_1}\right)^2 \text{ moles/cm}^2\text{-sec.} \qquad (3)$$

$$\text{with} \quad k = 10^{4.574-2.23(\frac{10^4}{T})}. \qquad (4)$$

---

1. P. O. Schissel & O. C. Trulson Technical Report No. C-26 Mass-Spectrometric Study of the Oxidation of Tungsten. Union Carbide Research Institute, October, 1964.

* This specifically excludes conditions where polymeric species (i.e. W_2O_6 and larger molecules) are important products, because definitive data[2] on these species were not obtained experimentally, or where gaseous diffusion rather than surface kinetics is rate-controlling.

There is a paucity of data on the oxidation of tungsten in oxygen at higher pressures under flow conditions where diffusion is not rate limiting. The present method of prediction agrees with the experimental results of Perkins et. al.[2] to ca. 50% at 2900°K and 0.1 to 3 torr O_2; at higher and lower temperatures the agreement is somewhat poorer, but still commendable, since the comparison represents an extrapolation of the mass-spectrometric results by four orders of magnitude in pressure with no adjustable parameters.

b. Molybdenum-Oxygen Reaction

Vapor species formed by the reaction of molecular oxygen with molybdenum have been identified and their intensities measured as a function of surface temperature and oxygen pressure over the range 1472°K to 2437°K and 10^{-6} to 3×10^{-4} torr O_2. The principal products are $MoO_3(g)$, $MoO_2(g)$, MoO(g), and O(g); the temperature dependences are shown in Figure A-11 where log (vaporization rate) vs. reciprocal temperature is plotted for each of the species at an incident oxygen flux of 4.7×10^{16} molecules/cm^2 sec. The most striking feature of these data is the MoO(g) intensity, which is linear on this plot over a 900°C temperature range. (Quantitative measurements on the analogous species WO(g) could not be made for the tungsten-oxygen reaction because the isotopes of the large mercury background occur at the same mass positions as WO.) The species O, MoO_2, and MoO_3 exhibit temperature dependences similar to those exhibited by O, WO_2, and WO_3 in the tungsten-oxygen reaction.

Pressure dependences were measured for each of the species at various temperatures. For MoO(g) and O(g), the order varies from 0.5 to 1, increasing with increasing temperature. For $MoO_3(g)$ the order varies from near 1.0 at 1811°K to near 1.4 at 2120°K; only one run was taken with MoO_2, this giving nearly first-order dependence at its temperature maximum.

Various kinetic models are being considered for this system. In view of its similarity in behavior to the tungsten-oxygen system, a "two-layer" model was considered first. Although the data have not been fitted numerically to the model, the O, MoO_2, and MoO_3 results probably can be explained on this basis. The MoO data are more difficult to explain; since temperature-saturation of this species is not observed, its temperature trend need not be interpreted on the basis of decreasing surface coverage.

---

2. R. A. Perkins, W. L. Price, D. D. Crooks, Lockheed Missiles and Space Co. [illegible], November 1[illegible].

c. Future Work

Measurements currently underway with beams of oxygen atoms (formed by cracking CO_2) indicate that these react with molybdenum to form $MoO_3(g)$ about 100 times as efficiently as does $CO_2(g)$; the rate of production of other molybdenum species is less affected. It is planned to continue these measurements and extend them to the CO_2-W system.

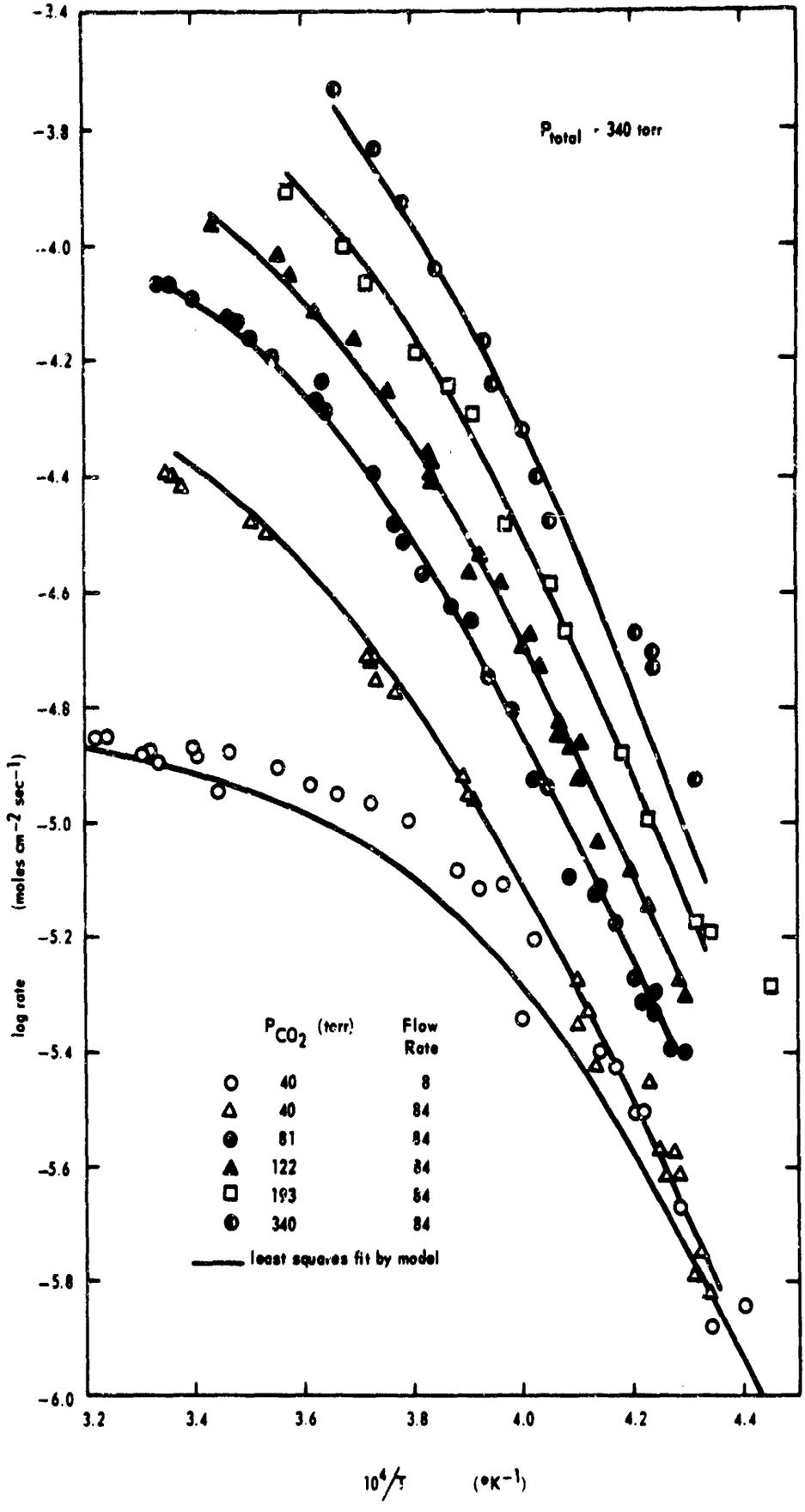

FIGURE A - 1 FIT OF MODEL TO CO_2/W REACTION RATE DATA

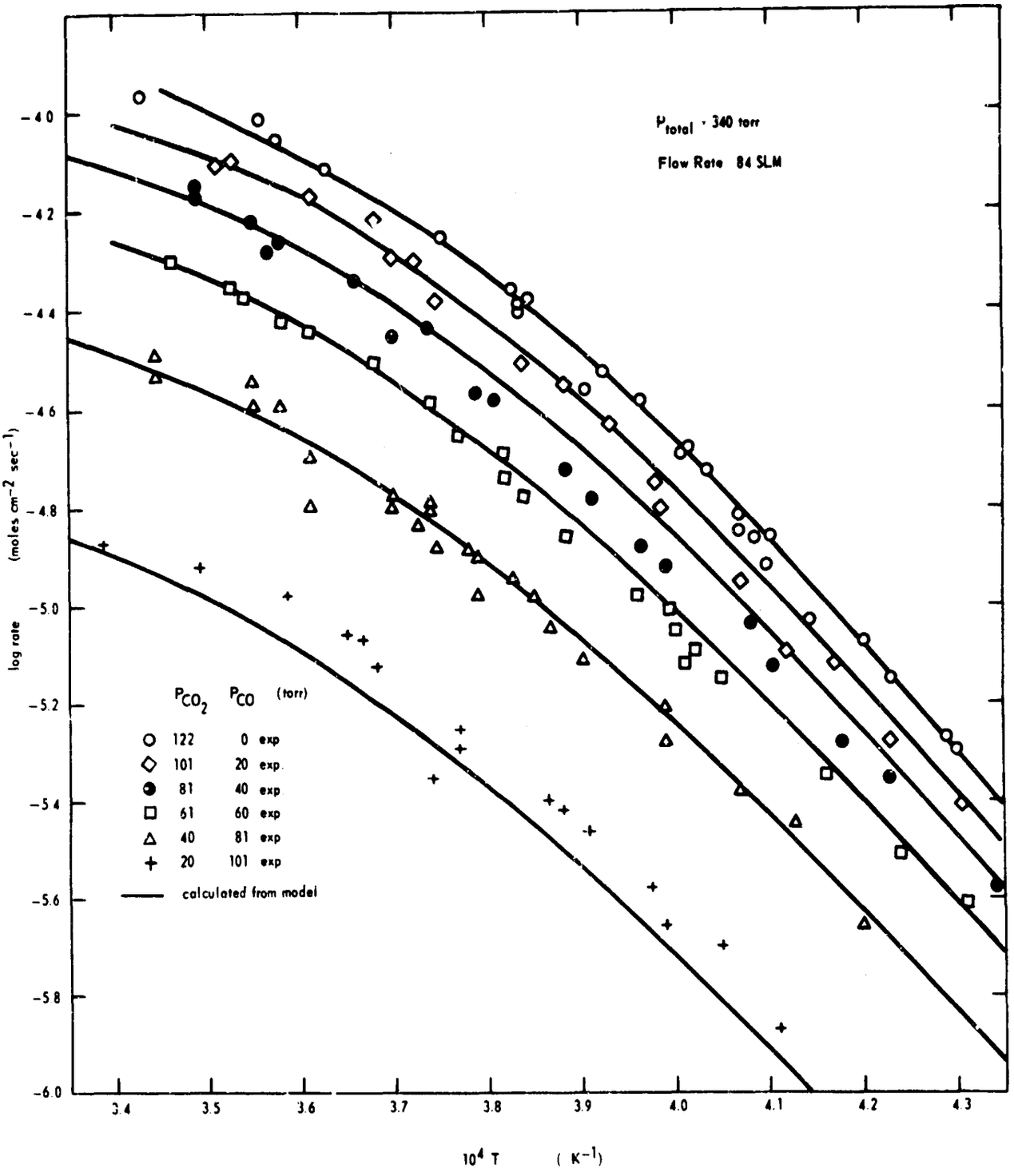

FIGURE A - 2 COMPARISON OF CALCULATED AND OBSERVED RATES OF CORROSION OF W BY CO_2/CO/Ar MIXTURES

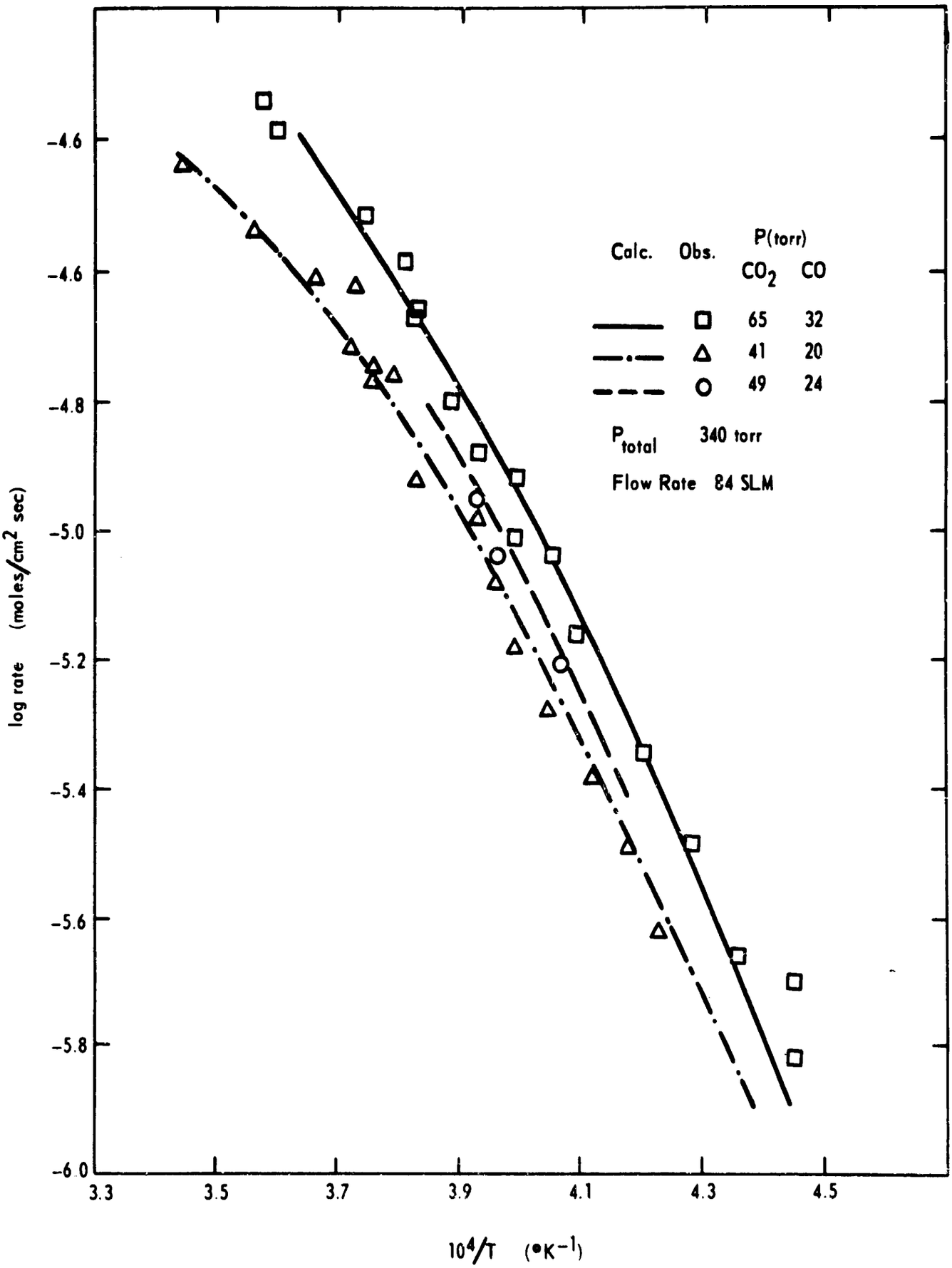

FIGURE A - 3 COMPARISON OF CALCULATED AND OBSERVED RATES OF CORROSION OF W BY $CO_2/CO/Ar$ MIXTURES: CO_2/CO_2 - 0.5

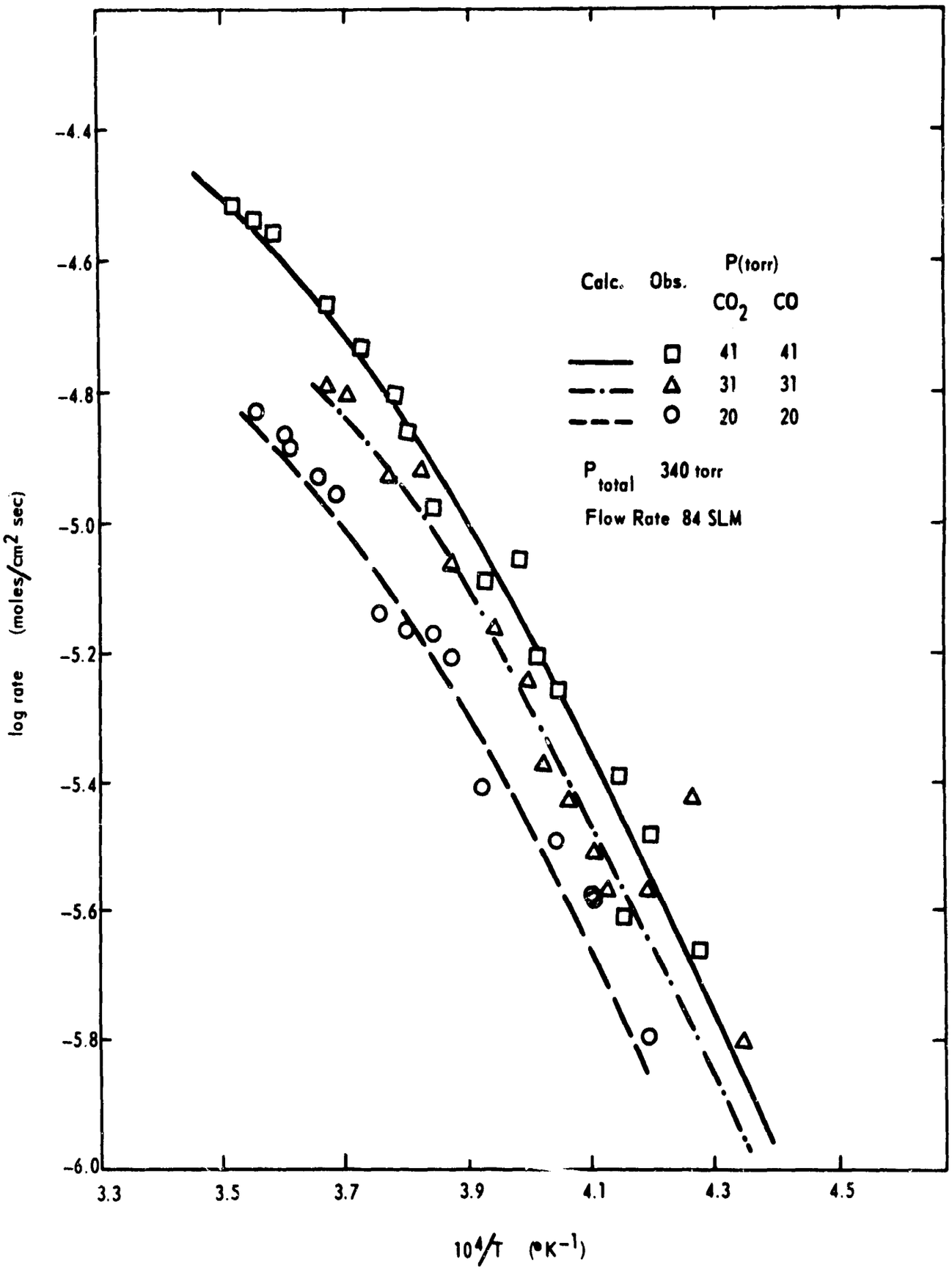

FIGURE A - 4 COMPARISON OF CALCULATED AND OBSERVED RATES OF CORROSION OF W BY $CO_2/CO/Ar$ MIXTURES: $CO/CO_2 = 1$

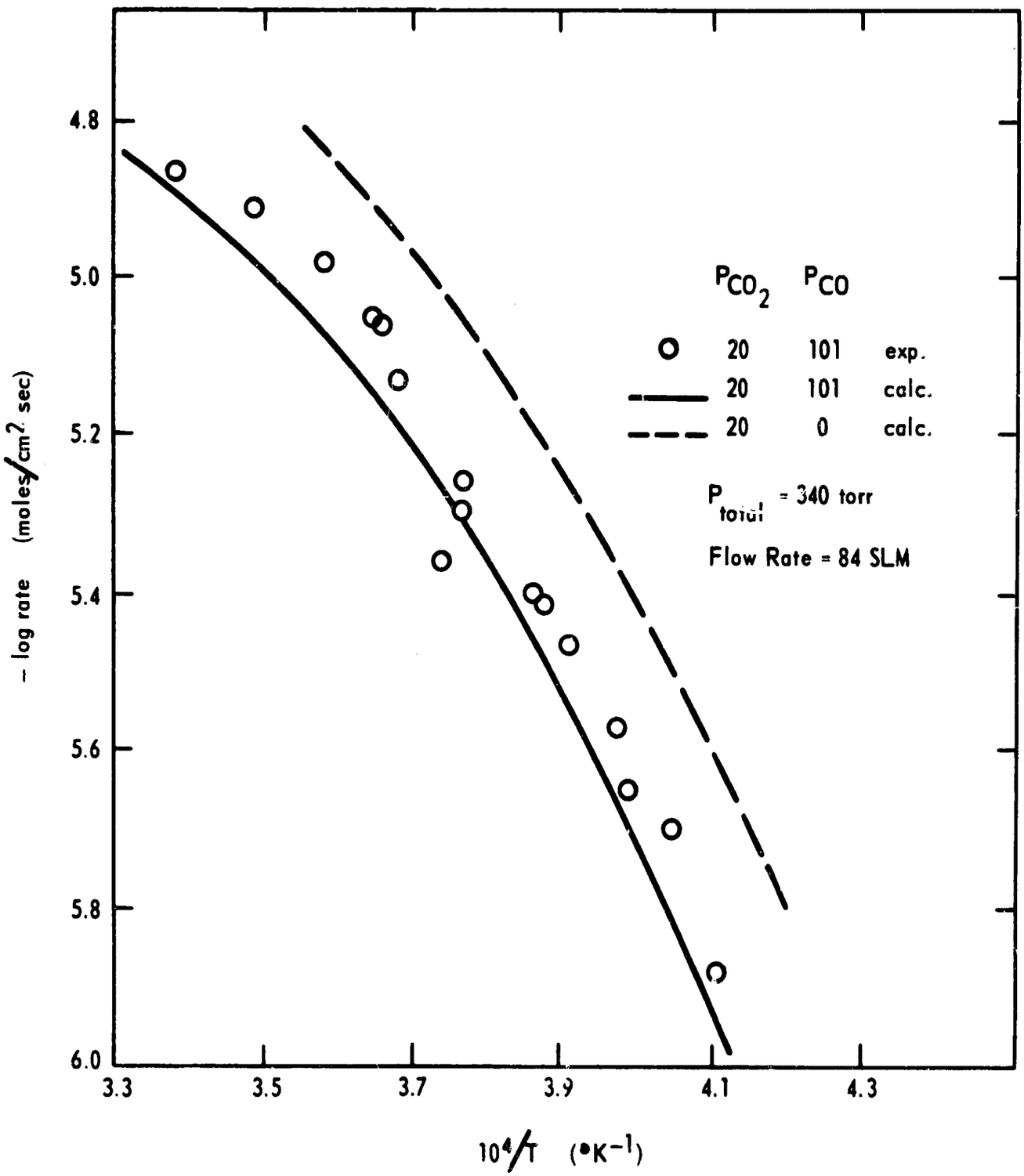

FIGURE A - 5 TEMPERATURE DEPENDENCE OF CORROSION OF W IN 20 TORR CO_2

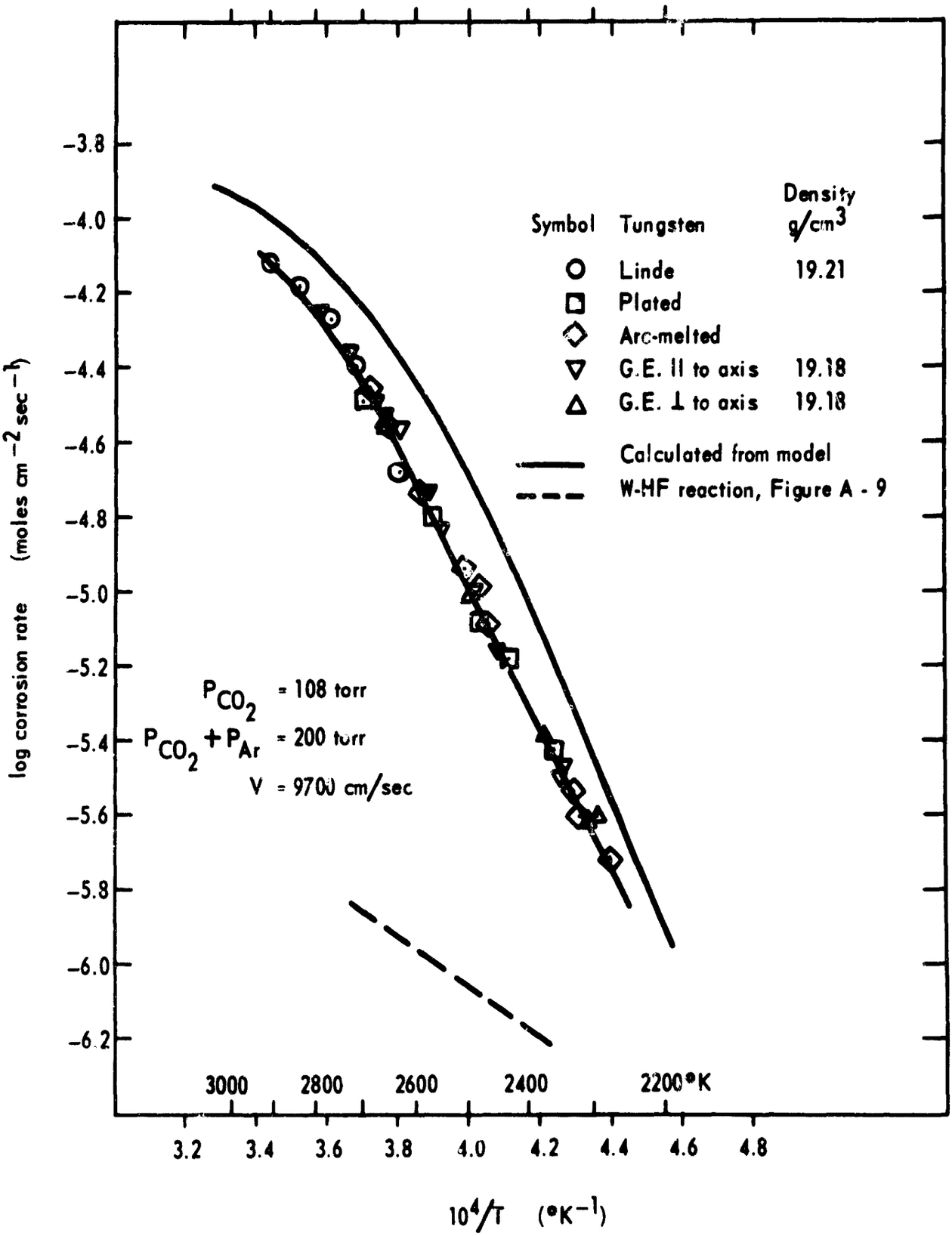

FIGURE A - 6 TEMPERATURE DEPENDENCE OF THE CORROSION RATE OF SEVERAL TUNGSTEN SAMPLES IN CO_2

FIGURE A - 7 COPPER INLET TUBE FOR HF REACTIONS

33X

A. Sandblasted

370X

B. Sandblasted

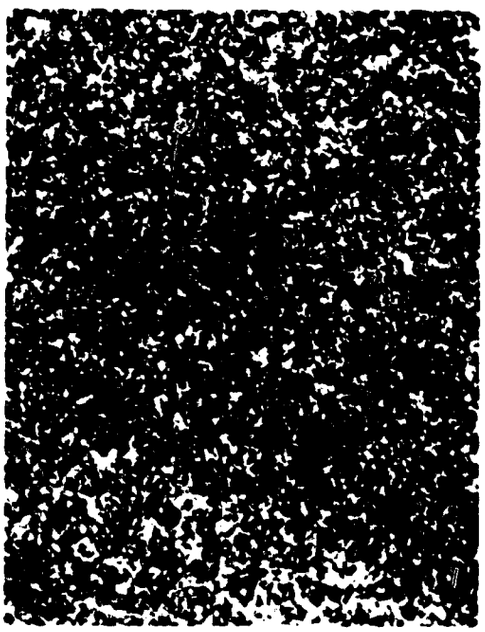

33X

C. Oxidized, 108 torr CO_2
4.0 min., 2350°K

370X

D. Oxidized, 108 torr CO_2
4.0 min., 2350°K

FIGURE A - 8 EFFECT OF SURFACE TREATMENT UPON EMITTANCE OF POLISHED G.E. TUNGSTEN 30A5

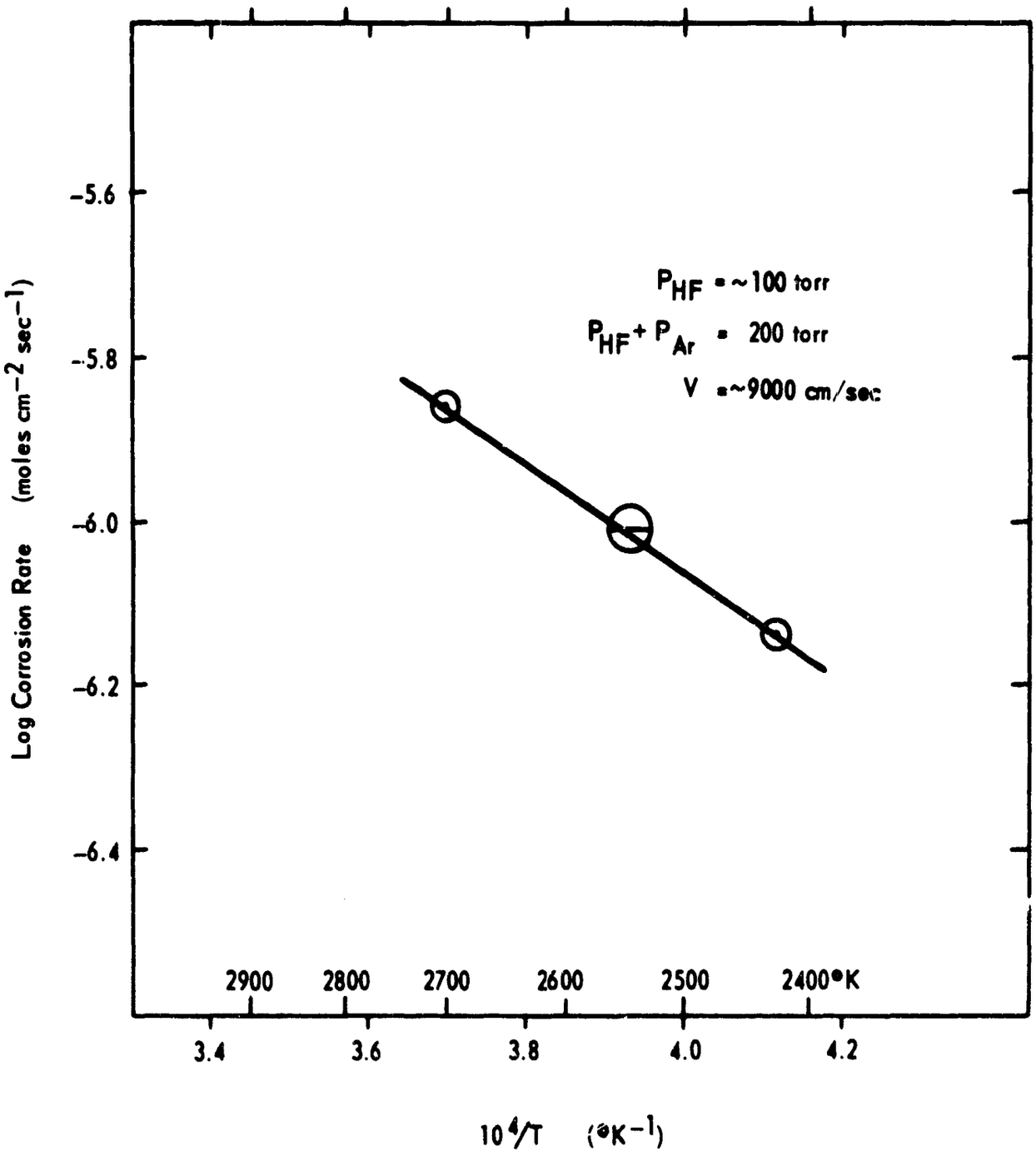

FIGURE A - 9 TEMPERATURE DEPENDENCE OF THE CORROSION RATE OF LINDE TUNGSTEN IN HF

$$\alpha \equiv \frac{1}{P_{mm}} 10^{7.845 - 3.147 \left(\frac{10^4}{T}\right)}$$

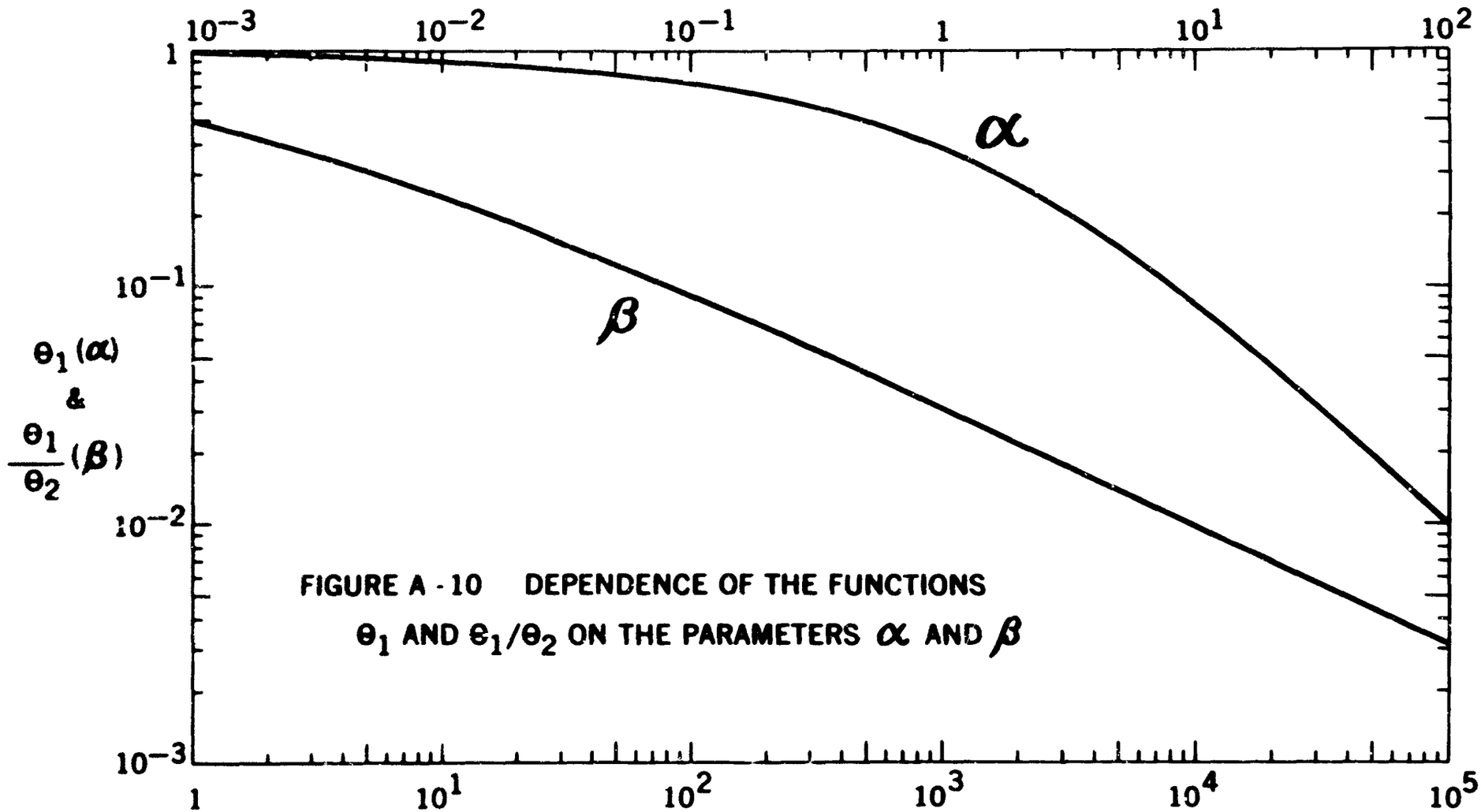

FIGURE A - 10 DEPENDENCE OF THE FUNCTIONS θ_1 AND θ_1/θ_2 ON THE PARAMETERS α AND β

$$\beta \equiv \frac{1}{P_{mm}} 10^{8.146 - 1.94\left(\frac{10^4}{T}\right)}$$

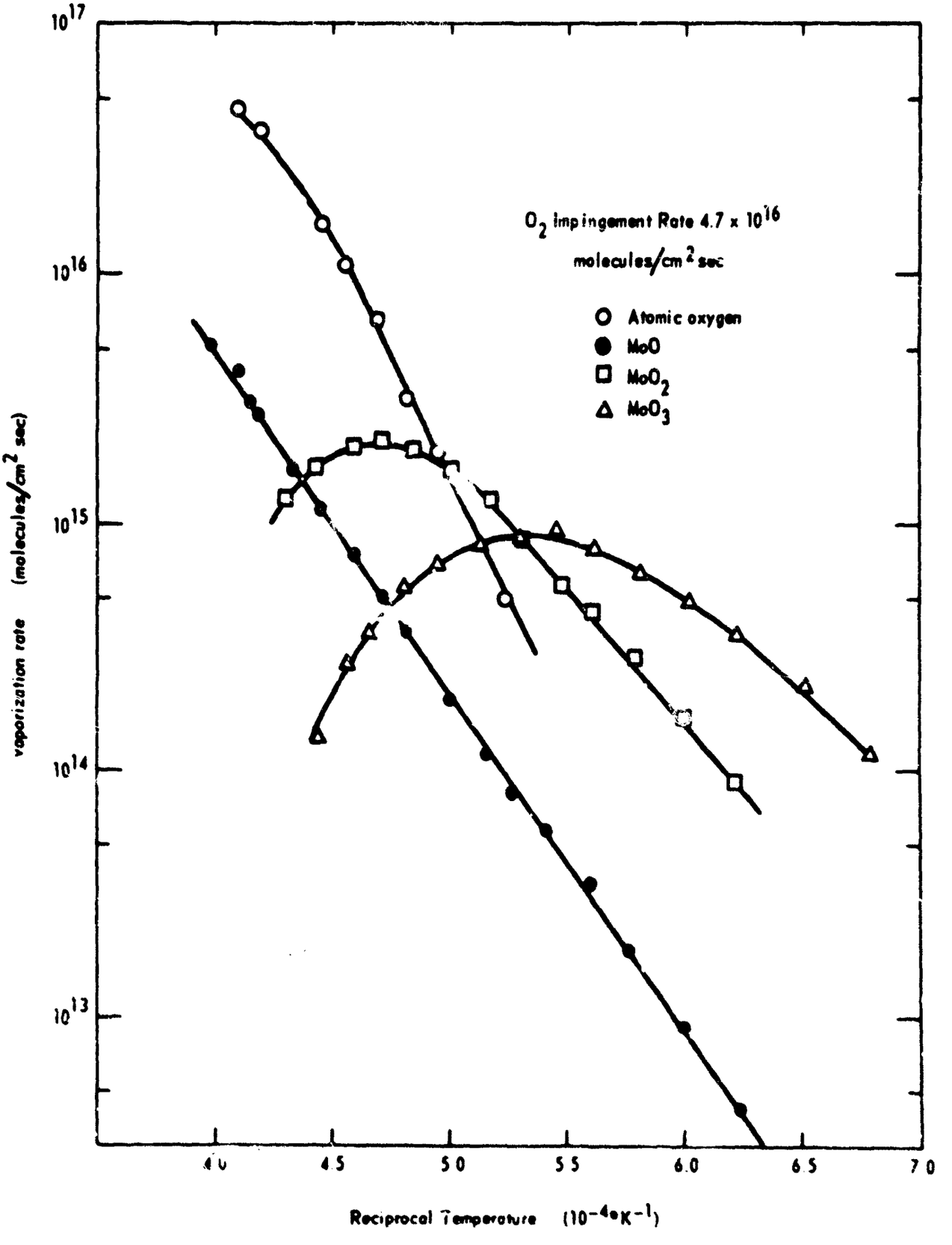

FIGURE A - 11 TEMPERATURE DEPENDENCE OF PRODUCT FORMATION IN Mo - O_2 REACTION

B. Physical and Mechanical Properties

1. High-Temperature X-ray Studies

Fred G. Keihn

As reported in the September 1964 QPR, boron is lost from the surface of NbB_2 and TaB_2 when they are heated in the x-ray vacuum furnace. To reduce this loss the high-temperature furnace for the Siemens diffractometer was filled with helium at higher than atmospheric pressure. This system was used to collect x-ray diffraction data on NbB_2 up to 1514°C from which lattice constants (Table B-I, still considered preliminary) were calculated by the least-squares program described in previous quarterly reports. Because of heat losses with the present furnace (designed for vacuum operation), higher temperature can only be obtained by reducing the helium pressure. Measurements at higher temperatures will be made by successively reducing the helium pressure until the surface of the sample is observed to lose boron.

Since the loss of boron from NbB_2 at 1000°C was not expected, an experiment was conducted by C. Trulson in which a sample of NbB_2 was heated on a tungsten strip in a mass spectrometer (10^{-6}-10^{-7} torr). A large signal at 84 mass units, believed to be $(HBO)_3$, was obtained from the sample at temperatures around 1000°C. Traces of water in the x-ray furnace and even smaller amounts of water in the spectrometer source furnace could explain the respective loss of surface boron in the x-ray sample and presence of $(HBO)_3$ in the mass spectrometer.

Table B-II gives lattice constant and thermal expansion data for TiB_2 up to 2041°C and compares these data with previous work by a somewhat different method on another sample. The agreement is excellent. Also, the agreement between lattice constants before and after the 2041°C run indicates that little boron was lost.

The thermal expansion of NbB_2 will be measured to the upper temperature limits of the present furnace, and the thermal expansion of TaB_2 will be determined using a helium atmosphere. Previously determined thermal expansion data for ZrB_2 will be rechecked to insure that loss of boron at high temperatures did not affect the results. A mass-spectrometric check of the species vaporizing from TiB_2 at 1000°C will be made.

Table B-I

Preliminary Lattice Parameters for NbB_2 As a Function of Temperature

Run*	Temp. °C	a (Å)	c (Å)
1	25	3.0866	3.3084
2	1012	3.1055	3.3401
3	25	3.0874	3.3082
4	753	3.0996	3.3312
5	1210	3.1104	3.3482
6	25	3.0870	3.3074
7	1514	3.1173	3.3574
8	25	3.0832	3.3107
9	1210	3.1102	3.3476
10	1514	3.1176	3.3579
11	25	3.0868	3.3090
12	753	3.0996	3.3300
13	1007	3.1055	3.3404
14	25	3.0870	3.3089

* One sample

Table B-II

Lattice Parameters and Thermal Expansion

For TiB_2 As a Function of Temperature

Run	Temp. °C	a(Å)	σ x 10^4*	c(Å)	σ x 10^4*	Relative expansion** x 10^3 $\frac{\Delta a}{a}$	$\frac{\Delta c}{a}$
1	25†	3.0291	2.1	3.2280	1.5		
		(3.0286)‡		(3.2282)‡			
2	1514	3.0630	8.1	3.2761	9.8	11.3	14.8
		(3.0629)		(3.2774)		(11.3)‡	(15.0)‡
3	1767	3.0684	19.5	3.2865	23.6	13.1	18.1
		(3.0694)		(3.2868)		(13.4)	(18.1)
4	2041	3.0767	3.9	3.2968	4.3	15.8	21.2
		(3.0771)		(3.2969)		(16.0)	(21.3)
5	25	3.0284	1.3	3.2283	1.6		

* σ-Standard deviation from the least-squares program.

† Run before heating, the runs are in sequence.

‡ The values in parentheses were obtained by C. Houska (QPR September 1964) by a somewhat different method. Houska gave no σ's.

** a and c measured at 25°C.

2. Elastic Properties — Robert Lowrie

Measurements of C_{11} have been successfully made on tungsten crystal L-2 from room temperature to 1800°C. These results together with the values previously measured (QPR June 1964) for C_{44} and $C_N = (1/2\ C_{11} + 1/2\ C_{12} + C_{44})$, yield the individual values of C_{11}, C_{12}, and C_{44} as functions of temperature to 1800°C. A report covering this work is being prepared.

A report has been prepared and will be issued shortly on the dynamic elastic properties of polycrystalline tungsten from 24° to 1800°C. Least-square equations have been calculated for the various elastic constants of our sample (99.4% dense) versus temperature and also for the constants of fully dense tungsten vs. T(°C), which are as follows:

$$G = 1.5893 \times 10^{12} - 14733 \times 10^{8}T - 2.448 \times 10^{4}T^{2}$$

$$L = 5.2415 \times 10^{12} - 3.7399 \times 10^{8}T - 4.598 \times 10^{4}T^{2}$$

$$K = 3.1224 \times 10^{12} - 1.7755 \times 10^{8}T - 1.333 \times 10^{4}T^{2}$$

$$E = 4.0761 \times 10^{12} - 3.5521 \times 10^{8}T - 5.871 \times 10^{4}T^{2}$$

$$\nu = 0.28247 + 6.1902 \times 10^{-6}T + 3.162 \times 10^{-9}T^{2}$$

Attempts have been made to measure the elastic constants of polycrystalline tantalum and niobium, but the transmission of ultrasonic pulses has been too poor in the specimens obtained from a commercial source to make meaningful measurements. The velocity of compressional waves in polycrystalline molybdenum has been measured from room temperature to 1760°C. However, difficulties have been encountered in making shear measurements over the same range, apparently as a result of the presence of small interfering echoes.

No further work on dynamic elastic properties is planned except as needed for studies of composite materials.

3. High-Temperature Creep of Refractory Carbides — Frederick G. Keihn

High-temperature creep has been followed as a function of stress at constant temperatures for three more large-grained polycrystalline TiC specimens. The starting materials for two of these, TiC-41 and TiC-43, were much purer than for previous specimens, but chemical analyses of the arc-fused boules are not yet

available. The other specimen, TiC-33, was made from the same materials as specimens TiC-32 and TiC-34, which are known (QPR September 1964) to contain fractional percentages of Zr and V. The creep rates were much larger for TiC-41 (Figure B-1) and TiC-43 (Figure B-2) than for TiC-33 (Figure B-3).

The creep rates are plotted in log-log form in Figure B-4, the stress having been calculated in each case from the applied total load and the changing cross section of the specimen as it deformed. Specimen TiC-33 showed a high stress dependence ($\sim\sigma^{10}$) comparable to the stress dependence reported in QPR September 1964 for a specimen, TiC-37, of equivalent purity. Specimens TiC-41 and TiC-43 showed the smaller stress dependencies $\sigma^{6.0}$ and $\sigma^{6.2}$, respectively.

Our extensive creep data on many TiC specimens are now being summarized and analyzed. One observation is that the plastic deformation of TiC is a very sensitive function of structure and impurities. This would suggest that the high-temperature mechanical properties of TiC specimens in general will also be highly dependent on their thermal and mechanical history.

Next quarter, the stress dependence for more TiC specimens of high purity will be determined, and a few creep tests will be made on TaC-HfC and TaC-ZrC solid solutions.

4. Steady-State Creep in Body-Centered Cubic Metals — Robert L. Cummerow

A set of six single-crystal Nb tensile specimens was received from Dr. E. Votava of Union Carbide European Research Associates. There are two specimens each for the principal crystallographic directions, [100], [110], and [111]. Since single-crystal specimens of tungsten are not yet ready, it was decided to make measurements on the niobium samples first and the tungsten second. In addition, Dr. Votava has made a careful study of the yield characteristics of niobium single-crystals at room temperature so that a correlation with Dr. Votava's work will be sought for high temperature, steady-state creep as a function of orientation.

This change of plans will necessitate consideration of the slip systems $\{110\}\langle 111\rangle$ rather than the systems $\{112\}\langle 111\rangle$ reported for tungsten in the QPR for September 1964. A modification of the tensile furnace is also

being made in order to accommodate Dr. Votava's samples, which were fabricated entirely by zone melting. In addition to the tensile creep experiments on these samples, resistance ratio measurements, x-ray orientation measurements before and after deformation, and metallographic tests to aid in slip plane determination will be made.

Apparatus - Satisfactory zone melting of 1/4-inch tungsten rod has not yet been achieved because the equipment for the automatic control of bombardment current in the electron beam zone refiner is not yet here. (It is on order and is expected to arrive momentarily.) If satisfactory samples cannot be refined from the 1/4-inch rod using this automatic control, the initial rod diameter will be reduced to 1/8 or 3/16 inch.

Very good results have been achieved in the electrolytic machining of 1/4-inch tungsten rod. A tensile specimen 4 inches long with a 5/8-inch gauge section in the middle and 1/4-inch long cylindrical knobs on each end has been produced. The surface is highly polished and regular. The sample was mounted horizontally in a small lathe and immersed in an aqueous solution of about 6% NaOH. A long, flat cathode of stainless steel was placed parallel to the cylindrical sample and the current density was maintained high enough to guarantee polishing action as determined visually. The sample was rotated at about 4 r.p.m. Stop-off lacquer was used to delimit the regions to be machined.

The various components of the tensile creep measurement system were tested together in a preliminary run. This test included the heater and heater power supply; a photo-tube temperature sensor, which controlled the sample temperature through an L and N recorder, magnetic amplifier and saturable core reactor; and a pumping system made up of one each of Varian sublimation and vacion pumps with a Linde liquid nitrogen cryosorption fore pump. Temperature calibration was afforded by an optical pyrometer sighting on a black-body hole in the sample. At 1865°C there was a variation of about 35°C along the 1/2-inch gauge section. This difference will be reduced. The temperature range covered was 1000 to 2000°C. Diffusion-limited creep in Nb will occur throughout this temperature range. The pressure in the cold chamber was 2×10^{-9} torr; at the highest temperature, 5×10^{-7} torr. The differential transformer, control unit, and recorder for measuring sample deformation were checked out separately. The equipment all functioned satisfactorily, and a complete set of experiments on the niobium samples will be attempted during the next quarter.

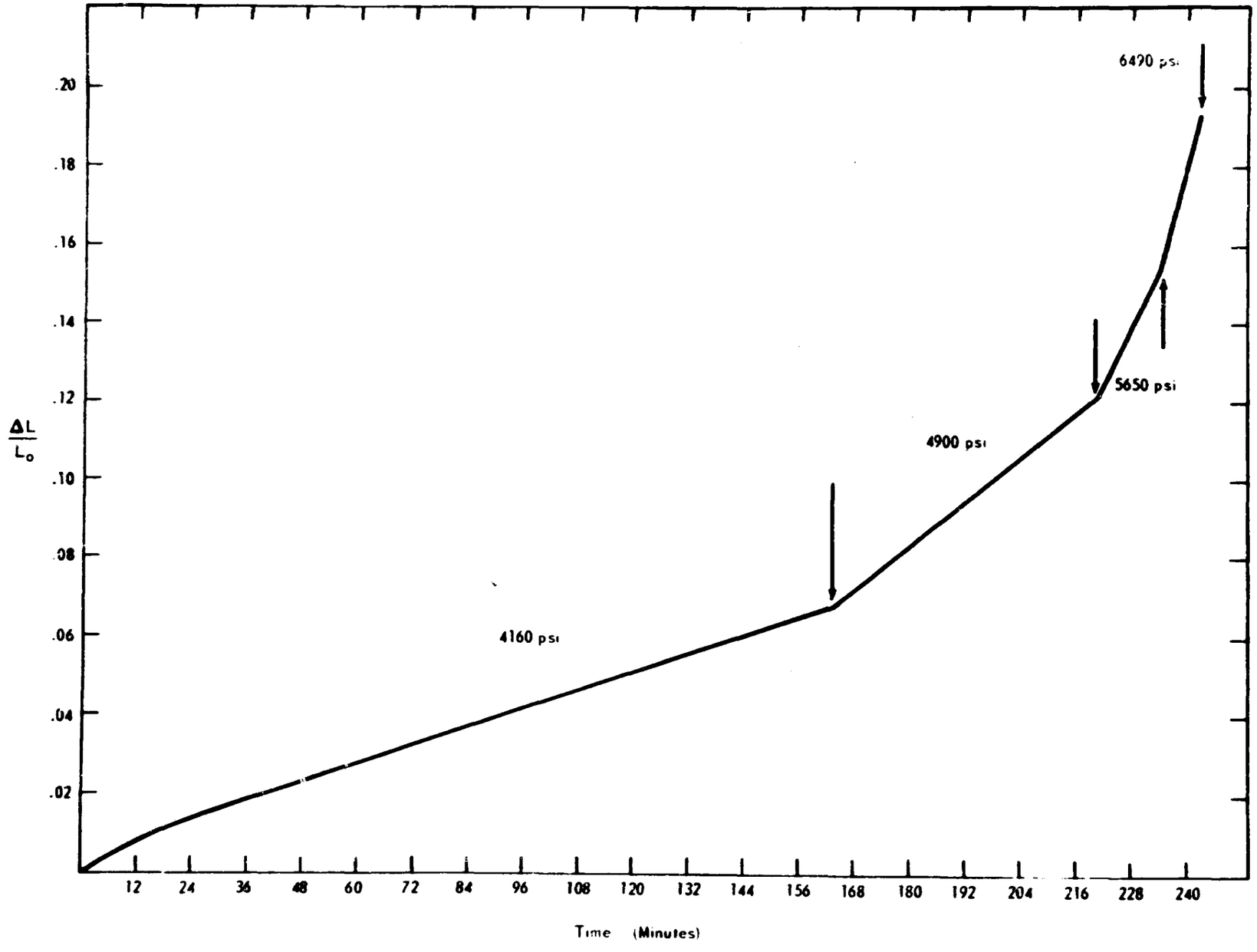

FIGURE B - 1 CREEP OF SPECIMEN TiC-41 AT 2240°K

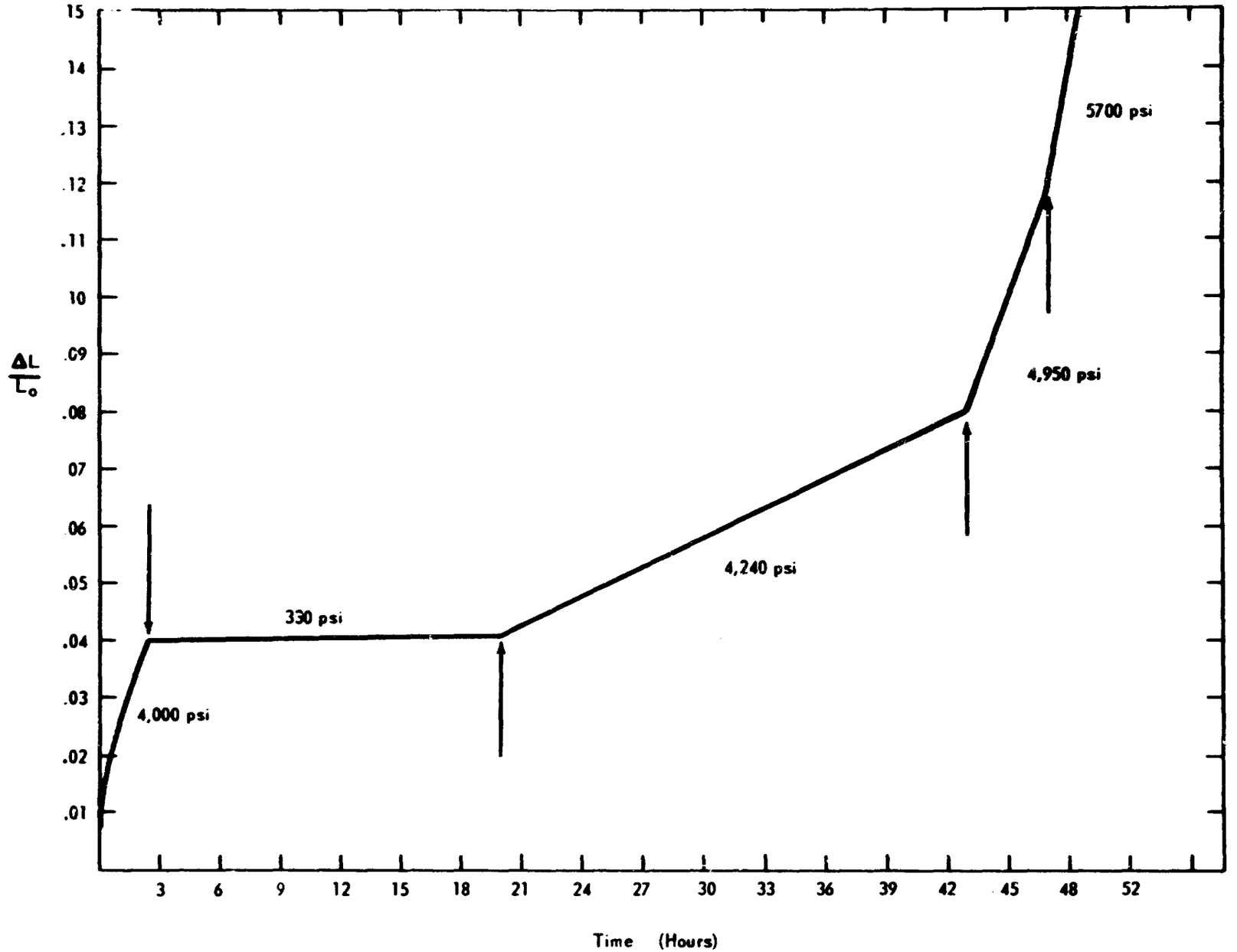

FIGURE B - 2 CREEP OF SPECIMEN TiC-43 AT 2184°K

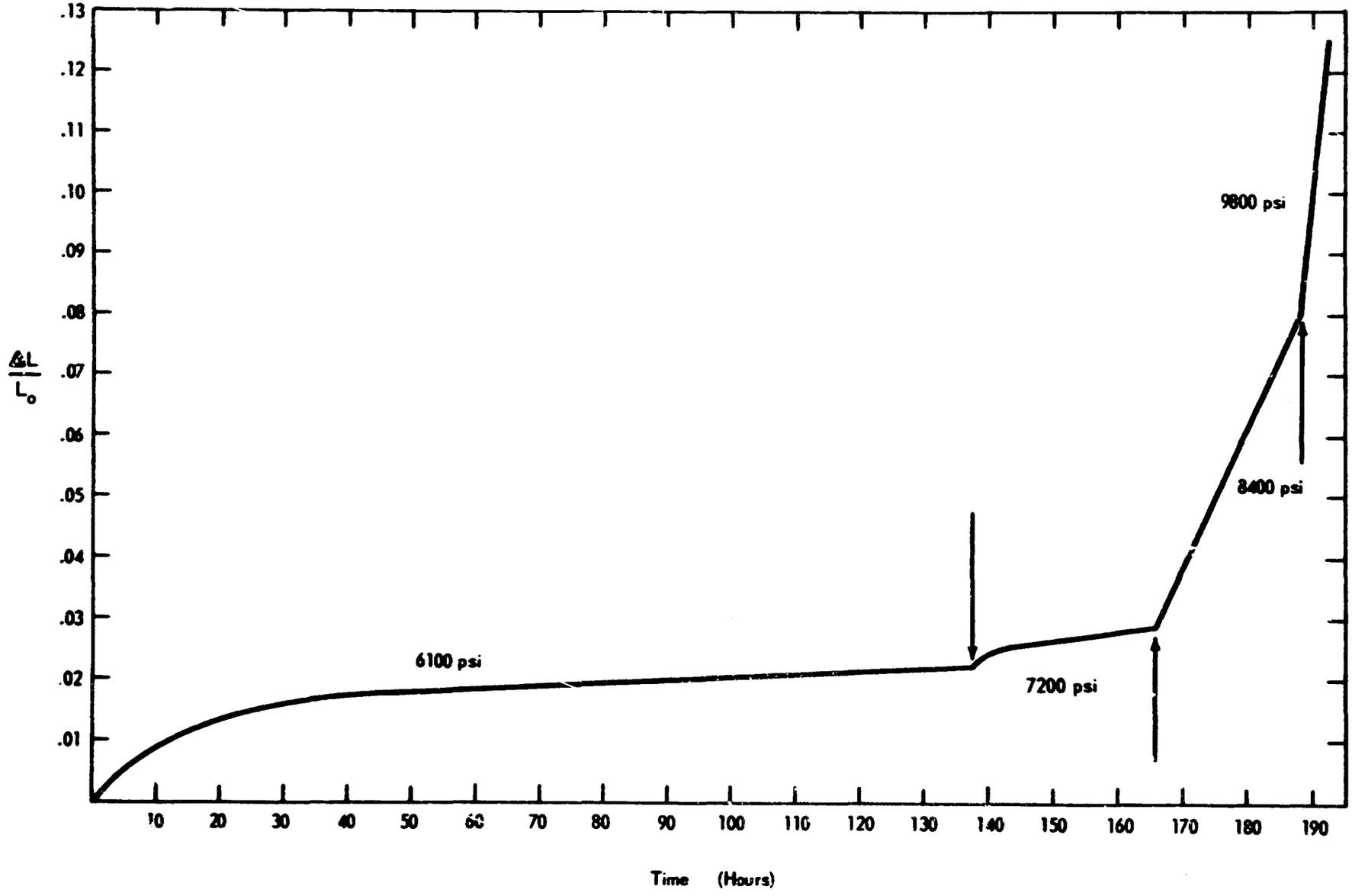

FIGURE B - 3 CREEP OF SPECIMEN TiC-33 AT 2231°K

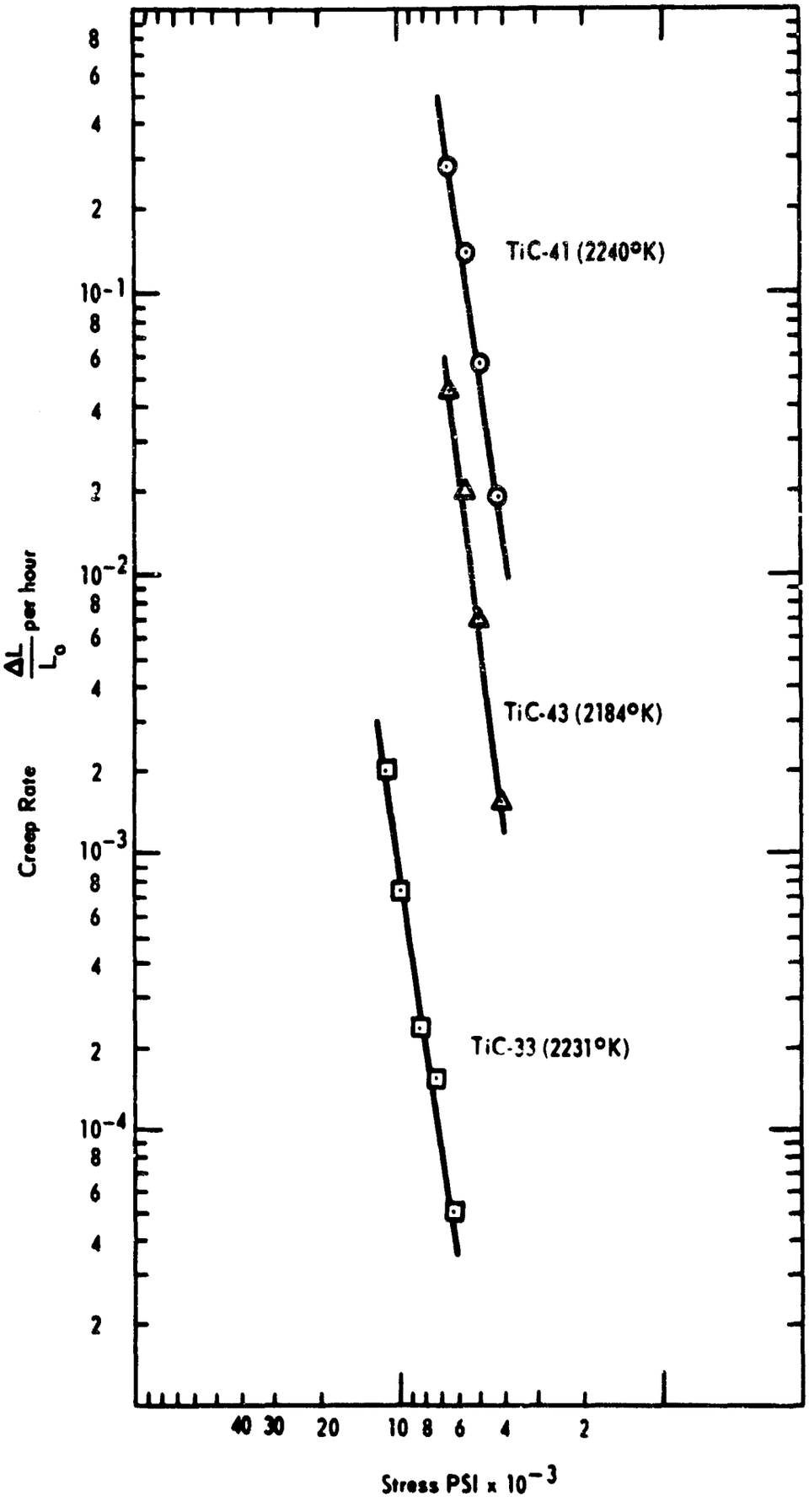

FIGURE B - 4 CREEP RATE VERSUS STRESS

C. Specimen Preparation and Characterization

1. Purification and Sample Preparation — I. Binder

Powders of TaC, ZrC, and TaC-ZrC and TaC-HfC solid solutions have been prepared and purified for work on skeletal carbides. The powders are being used to prepare skeletal carbide composites as reported in Section D-1 and for preparing arc-fused specimens for wetting studies relating to the infiltration process.

Polycrystalline molybdenum and niobium rods, 18" long and 3/4" in diameter, for the attempted acoustical measurements of elastic properties were annealed in the equipment usually used for zone sintering.

2. Analytical Research — G. J. McKinley, H. F. Wendt

a. Determination of Boron - The pyrohydrolytic determination of boron in zirconium diboride and titanium diboride has been described (QPR September 1964). During this quarter the technique has also been successfully applied to the diborides of tantalum and niobium, and, with some modifications, to hafnium diboride as well.

Samples of the diborides of niobium, tantalum, and hafnium were obtained and reduced to -200 mesh. The niobium and tantalum diborides were analyzed for boron by pyrohydrolysis and by the routine peroxide fusion method. The results (Table C-I) indicate greater boron recovery by pyrohydrolysis than by the peroxide fusion. Moreover, the low total analyses shown in Table C-II suggest that the fusion in fact does give incomplete boron recovery.

Several modifications in procedure were necessary for complete boron recovery from hafnium diboride: (1) The furnace temperature was increased to 1400°C (pyrohydrolysis at 1200°C and 1300°C gave improved but incomplete recoveries); (2) a zircon boat (Leco No. 528-57) was substituted for the platinum boat, since the latter deteriorated badly at temperatures greater than 1100°C; (3) oxygen was introduced into the steam generator at a rate of approximately 5 ml per minute in order to maintain a steady flow of steam through the combustion tube; (4) the time of distillation was increased to two hours; (5) the potentiometric end points were calculated by use of the second derivative

method, since the volume of solution, mannitol concentration, and ionic concentration differed from the fixed conditions which had been established for routine determination.

The results (Table C-III) are in good agreement with the results obtained by use of the routine peroxide fusion method. Quantitative spectrographic analysis of the residues from the pyrohydrolysis of the hafnium diboride indicated less than two parts of boron per thousand parts of the boron present in the original sample.

Although only hafnium diboride was run using the several modified conditions described above, these conditions would appear to be desirable for routine use with all samples. It was found that continuous operation of the furnace at 1400°C shortens the life of the quartz combustion tube considerably (after ten runs at this temperature it had deteriorated badly), but the zircon boat performed satisfactorily.

A research report entitled "The Determination of Boron in Refractory Borides by Pyrohydrolysis" has been written and approval for publication requested.

Table C-I

Comparison of Pyrohydrolysis and Fusion Methods for Boron Determination on Diborides of Niobium and Tantalum

(in weight percent Boron)

	Pyrohydrolysis Method		Routine Peroxide Fusion Method	
	NbB_2	TaB_2	NbB_2	TaB_2
	19.66	11.42	19.42	11.06
	19.60	11.43	19.32	11.02
	19.65	11.42	19.22	11.06
	19.67	11.42	19.31	11.20
	19.58	11.42	19.30	11.05
	19.70	11.43	19.14	11.15
Mean	19.64	11.42	19.28	11.09
Std. Dev.	0.04	0.006	0.10	0.07

Table C-II

Composition of Metal Borides

(in weight percent)

Sample	Metal	Boron[a]	Carbon	Nitrogen	Oxygen	Total Impurities[b]	Total Analysis
NbB_2	78.87	19.28	0.23	< 0.01	0.41	0.50	99.29
TaB_2	88.10	11.09	0.05	< 0.01	0.15	0.14	99.53

[a] Boron determined by routine peroxide fusion procedure.

[b] Total impurities determined by quantitative spectrographic analysis.

Table C-III

Comparison of Pyrohydrolysis and Fusion Methods for Boron Determination in Hafnium Diboride

(in weight percent Boron)

Run No.	Pyrohydrolysis at 1400°C	Routine Peroxide Fusion Procedure
1	10.32	10.22
2	10.28	10.18
3	10.34	10.20
4	10.31	10.20
5	10.31	10.17
Mean	10.31	10.19
Std. Dev.	0.02	0.02

b. Determination of Free Carbon - Some additional work on the determination of free carbon in refractory metal carbides has been completed. These determinations are made here by a modified Kriege procedure (QPR June 1963) designated in this and previous reports as the UCCND method. The method requires dissolution of the carbide by first adding 15 ml of concentrated nitric acid and then concentrated hydrofluoric acid dropwise until re-

action ceases. The insoluble free carbon is removed by filtration and determined as carbon dioxide by combustion.

Recently a method for the determination of free carbon in hafnium carbide was published[1] which differs basically from the UCCND method in two ways – (1) The amounts and the order of addition of acids are changed, i.e. the carbide sample is treated with 20 ml of hydrofluoric acid (rather than nitric), after which nitric acid (rather than hydrofluoric) is added dropwise until reaction ceases; (2) the residue is washed with a hot 10% sodium hydroxide solution before combusting the separated free carbon. The second change was made in the effort to eliminate "high and erratic results" obtained when the Krieger method was applied to hafnium carbide of very low free carbon content. The irregular results were attributed to the presence in the residue of dark red, translucent particles, which could be dissolved in the 10% sodium hydroxide solution.

Feick and Giustetti suggested that the red residue represented combined carbon which is incompletely oxidized during acid treatment, and that the amount of such residue depends on the particle size of the carbide and on the details of the acid treatment.

However, our experience with the UCCND method is that using a large amount of hydrofluoric acid initially and then adding nitric acid dropwise in a lesser amount promotes the formation of a reddish material which, if carried through subsequent steps of the analysis, causes high and erroneous results.

Experiments designed to confirm this conclusion in detail were performed. Samples of zirconium carbide and hafnium carbide (-200 mesh) were analyzed for free carbon by three procedures - (1) the UCCND method; (2) the UCCND method with reversed acid addition; (3) the Feick-Giustetti method. In procedure No. 2 only the amounts and order of addition of acids were changed, i.e. the sample was dissolved by treatment with 15 ml of hydrofluoric acid and dropwise addition of nitric acid until reaction ceased. The Feick-Giustetti method was followed faithfully except for the carbon dioxide measurement, which was gravimetric instead of conductometric.

---

(1) Feick, G., Giustetti, W., Anal. Chem. 36, 2198 (1964).

The results (columns 1 and 2 of Table C-IV) indicate that the nitric acid must be added first to avoid incomplete oxidation of the combined carbon and consequent formation of organic intermediates. Although these organic products may be removed by washing the filtered residue with sodium hydroxide solution, (column 3), our method (UCCND) of dissolution apparently prevents their formation. It has also been noted that a sufficient excess of nitric acid is capable of destroying any organic intermediates formed by reversing the preferred order of acid addition.

Table C-IV

Effect of Reversing the Acid Additions in UCCND Method and Counterbalancing Effect of the Feick-Giustetti Caustic Wash

(Results in percent free carbon)

Sample		UCCND Method	UCCND Method With Reversed Acid Addition	Feick-Giustetti Method
ZrC		0.08	3.39	0.09
		0.11	4.12	0.05
		0.07	3.82	0.08
	Mean	0.09	3.78	0.07
	Range	0.04	0.73	0.04
HfC		0.07	3.07	0.12
		0.07	2.49	0.09
		0.11	2.74	0.08
	Mean	0.08	2.77	0.10
	Range	0.04	0.58	0.04

A manual of our procedures for analysis of the refractory carbides and borides is being prepared.

D. Composites

The materials under consideration here – skeletal carbide composites – consist of two interlocking continuous phases, one a refractory carbide and the other a metal, and are designed to be superior in low-temperature properties to the refractory carbide itself, while maintaining its desirable high-temperature properties even though the metal may melt or vaporize. Such behavior, as measured by transverse rupture strength, has now been found for TaC-Ag composites.

1. Preparation — Ira Binder

The preparation of skeletal carbide composites was continued, with TaC, ZrC, and carbide solid solutions based upon TaC as the primary hardmetal skeletons. Work was concentrated on silver and silver alloys as infiltrants, since the carbide skeleton is not disrupted when the infiltrated silver is vaporized, whereas nickel-infiltrated TaC loses practically all its strength in the neighborhood of 1400°C. This problem with the original nickel infiltrant was investigated, and a study of the infiltration of TaC with "TaC-saturated" nickel was begun.

TiC-Ag Skeletal Carbides - Changes in the heating time and temperature have led to large improvements in the infiltration of TaC with silver. Several minutes at temperatures of 1400-1420°C was best. The occurrence of irregularly infiltrated regions, which may be partially due to non-uniformity of the hot-pressed TaC skeletons, can be reduced considerably by adding a small amount of nickel (less than 2 wt.% of the silver) to enhance wetting. Nickel by itself reacts, causing disruption of the carbide-carbide bonds at temperatures in the range of 1400°C, but a small amount in solution in the silver appears to assist the wetting process and to aid infiltration without damaging the TaC skeleton. Silver-infiltrated TaC specimens, when diamond-ground, show many small silvery spots and short lines, uniformly distributed over the surface. This indicates that the silver is filling the fine continuous porosity in the original skeleton without disrupting it or closing off its pores.

One method of determining the utility of an infiltrated composite at elevated temperatures is to check both the appearance and the properties of the skeleton after complete vaporization of the infiltrant at or above the projected

service temperatures. For our first trials the infiltrated bars were heated rapidly in the hot press, in a graphite die without pressure, to temperatures above 2000°C. After cooling to room temperature, silver-infiltrated TaC specimens so treated to evaporate the silver had substantially the same strength, density, and resistivity as the original hot-pressed TaC. There was no measurable change in any dimension, further indicating no real solution of TaC in the silver during infiltration or infiltrant removal, since any such solution and reprecipitation would have led to shrinkage and consequent densification. The transverse rupture strength of the TaC skeleton (Ag vaporized) is reported in greater detail below, in Section D-2.

TaC-Ni Skeletal Carbides - The transverse rupture strength of the TaC-Ni composites is high at room temperature but drops drastically at 1400°C. Furthermore, when the TaC-Ni composite is heated to high temperatures (over 2000°C) to drive off the nickel, the carbide skeleton remaining is porous and friable and easily broken by hand. The carbide-carbide bonds are evidently disrupted by the nickel at temperatures at and above its melting point.

This disruption should be minimized by pre-saturating the nickel infiltrant with TaC and using the "TaC-saturated" nickel to infiltrate the carbide skeleton. The solubility of TaC in molten nickel* has been studied by reacting varying amounts of TaC with Ni at 1475°C. TaC powder (+ 200 mesh) was placed on top of lightly compressed nickel powder in a recrystallized alumina boat and then heated in a ceramic tube furnace, in a purified flowing argon atmosphere. One run was made in a graphite crucible, with a Ni + 20 wt.% TaC (i.e., 20 wt.% of the amount of nickel) composition.

The photomicrographs of Ni + 1% TaC (Figure D-1A) show only a porous single phase with no structure that could be related to TaC. The Ni + 10% TaC (Figure D-1B) shows many clear areas, some small inclusions which may be alumina entrapped in pores during grinding, and several areas with a Widmanstätten type of

---

* According to R.P.H. Fleming [Powder Metallurgy, 12, 179 (1962)] the solubility of tantalum carbide in nickel has been determined by R. W. K. Honeycombe [Proc. Aus. Inst. Min. Met., 128, 227 (1942)] and R. Edwards and T. Raine [Plansee Proc., p. 232, (1952)]. We have not yet received the last two references but Fleming claims less than 5 wt.% solubility of TaC in Ni for a compact sintered at 1350°C.

phase. A similar phase is visible throughout the Ni + 20% TaC (Figure D-2A). With Ni + 50% TaC (Figure D-2B), there is no longer a Widmanstätten phase, but instead many sharp-edged, rectangular prisms of TaC. Similar structures, with larger fractions of TaC, are seen in Ni + 75% TaC (Figure D-3A) and Ni + 100% TaC (Figure D-3B).

A photomicrograph (Figure D-4) of the specimen of Ni + 20% TaC heated in a graphite crucible shows a considerable quantity of platelike graphite inclusions. The long continuous lines are polishing scratches, rather than the structure visible in the Ni + 20% TaC melted in alumina.

Further Ni + TaC compositions between 20 and 50 added wt.% TaC will be made and studied to determine the composition at which discrete TaC particles begin to be seen. It should be noted that all the Ni-TaC compositions melted in this series retained a considerable ductility, despite the presence of hard second phases. All of the above compositions were cut by hand with a hacksaw before metallographic examination and could be deformed at room temperature by hammering.

The Ni + 20% TaC mixture (previously melted) is being used to infiltrate TaC skeletons. The mixture infiltrates readily, and rupture strength measurements are being made.

Other Skeletal Carbides - Hot-pressed ZrC bars (80-90% of theoretical density) made from purified ZrC powders have been infiltrated with nickel or with silver, but with irregular success. Sometimes the specimen infiltrated completely, but sometimes only a shallow surface layer seemed to be affected. Perhaps the pores in this material are often not continuous, despite the use of powders coarser than those used to produce TaC skeletons. In addition, despite purification, the ZrC is less pure than the TaC, which may lead to reactions causing a sealing off of interconnected pores. More reproducible porous skeletons will be sought by adding coarser particles to control the powder particle sizing. Further work on ZrC-based composites is desirable because they may well have better resistance to high-temperature corrosion than TaC and NbC composites have.

An additional means of achieving skeletal strength at very high temperatures, and also of making use of any possible advantage derived from the Group IV carbides, is the use of carbide solid solutions. It has long

been known that the TaC-HfC and TaC-ZrC systems show melting point maxima at ratios of approximately 4/1. Hardness and strength properties may also maximize at the same compositions. Batches of 80 TaC/20 HfC, 90 TaC/10 HfC, 80 TaC/20 ZrC, and 90 TaC/10 ZrC have been prepared and used to make both transverse rupture strength specimens and infiltration blanks. The first infiltration experiments with these compositions show behavior similar to that of TaC, indicating that essentially continuous fine porosity can be achieved reproducibly for these solid solution carbides.

Specimen Pressing - Isostatically pressed cylinders of TaC, ZrC, and NbC have been infiltrated successfully with 20 percent of nickel. In each case, the pressed and pre-sintered cylinder was of lower density than the skeletons prepared by hot pressing. Some shrinkage occurred during the infiltrations, indicating liquid phase sintering at the infiltration temperature of approximately 1475°C. To provide a denser and stronger hardmetal skeleton without recourse to excessively high processing temperatures, isostatic pressing of TaC mixed with a small amount (1 percent by weight) of nickel was studied. Furnace heating of one such specimen produced a body with a density 76 percent of the theoretical density for TaC. This cylinder was then infiltrated with 10 percent nickel, indicating that the pores of the partly sintered body were still essentially continuous. This procedure will be continued using metals such as silver both as sintering aids and as infiltrants.

It has been found that hot-pressed specimens will not infiltrate properly if they have been overheated enough to react with the graphite hot-pressing die. This is apparently caused by graphite platelets introduced into the carbide skeletons and by the disruption of the continuous network of fine pores. While this effect can best be seen with such a combination as TaC + Ag, it apparently can happen with any carbide + metal infiltration system. On this basis, the good purity of the TaC being used in this work can be a considerable advantage, since there is little free carbon in the original carbide powders.

Future Work - Work during the next quarter will be concentrated on infiltration of TaC with "TaC-saturated" nickel, the use of silver alloys as infiltrants, the preparation and infiltration of ZrC specimens with continuous

porosity, the use of TaC/HfC and TaC/ZrC solid solutions for the carbide skeletons, and isostatic pressing of larger composite bodies.

2. Mechanical Properties — Frederick G. Keihn

The transverse rupture strength of silver-infiltrated TaC has been measured up to 1800°C using the argon-atmosphere carbon tube furnace and loading system described in the September 1964 QPR. In addition to TaC-Ag specimens, strength measurements were also made on infiltrated specimens from which the silver had been evaporated leaving only the TaC skeleton. TaC-Ag composites and TaC itself (QPR September 1964) are compared in Figure D-5. The attractive feature for the composite is that it is generally stronger than the original TaC from room temperature to about 1400°C and comparably strong at 1800°C, only the 1600° point being unfavorable. The skeletons from which the Ag has been evaporated are comparable in strength to the original TaC. The infiltration and the subsequent vaporization of the silver apparently do not disrupt the TaC grain-to-grain bonds. This is what we hoped for. The need now is to further improve the room temperature strength – as is probably possible, for example, by replacing silver with silver alloys.

Specimens of nickel-infiltrated TaC from which the Ni had been vaporized were too weak even to be measured in the transverse rupture machine. The nickel-infiltrated TaC composites also do not have the desired strength at high temperatures (above 1400°C), and no further work will be done on them. We hope the mechanical properties of TaC infiltrated with "TaC-saturated" nickel will be good, however, but they still have to be investigated.

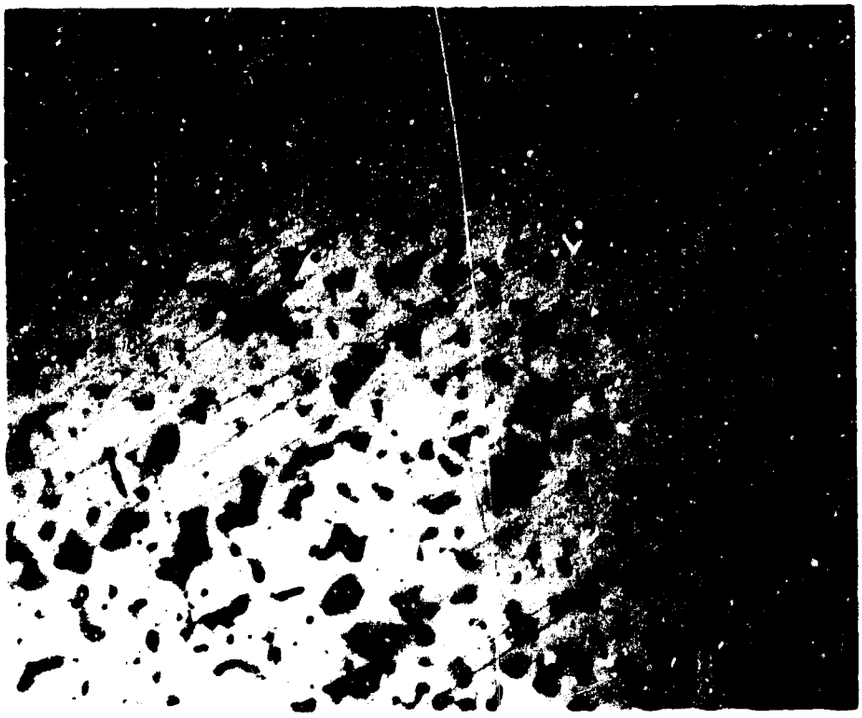

A. Ni + 1% TaC 300X

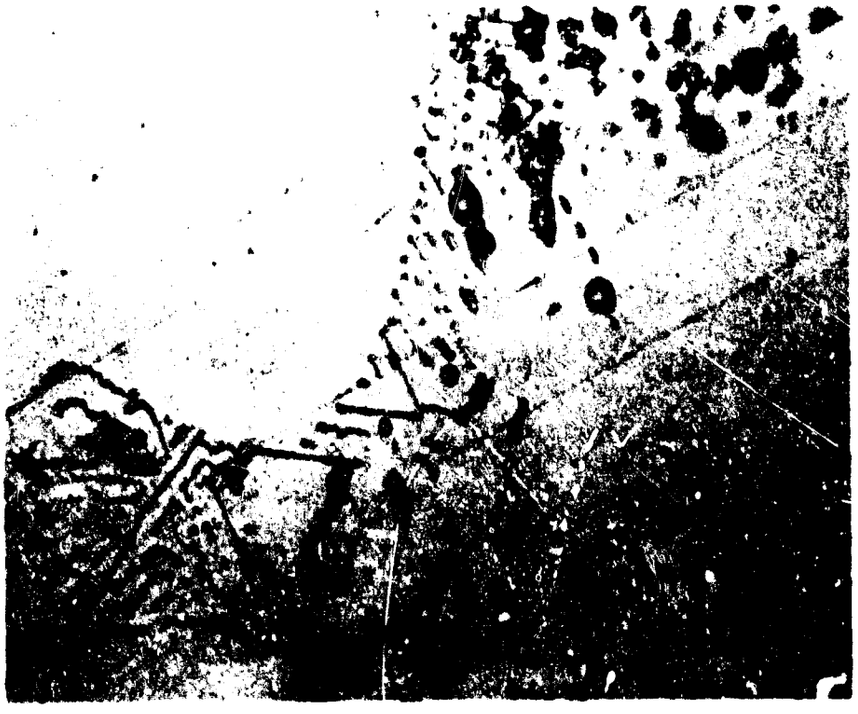

B. Ni + 10% TaC 300X

FIGURE D - 1 SOLUTION OF TaC IN NICKEL

A. Ni + 20% TaC 300X

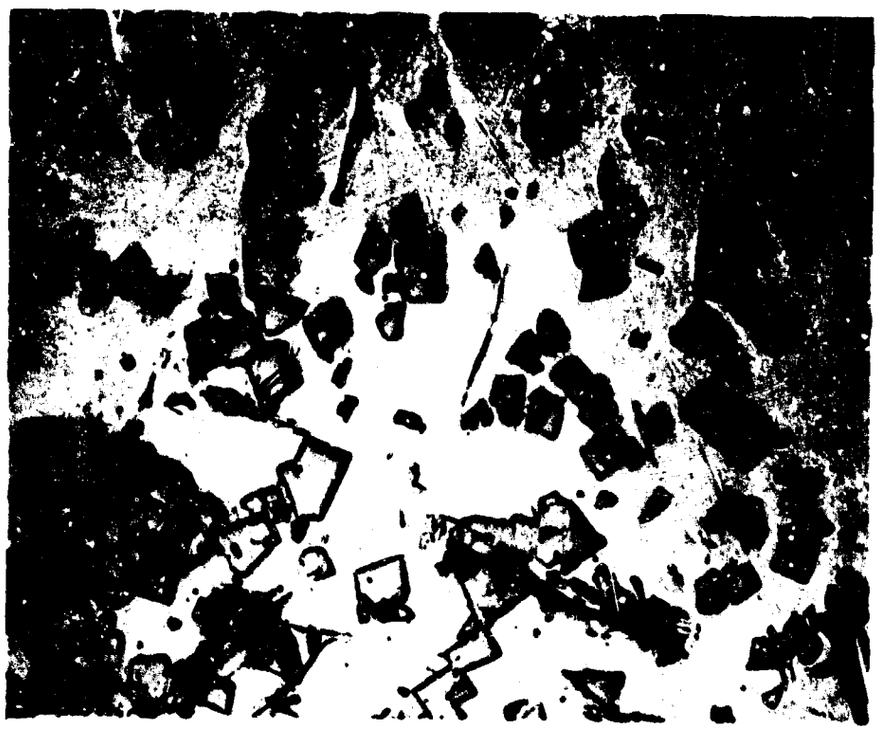

B. Ni + 50% TaC 300X

FIGURE D - 2 SOLUTION OF TaC IN NICKEL

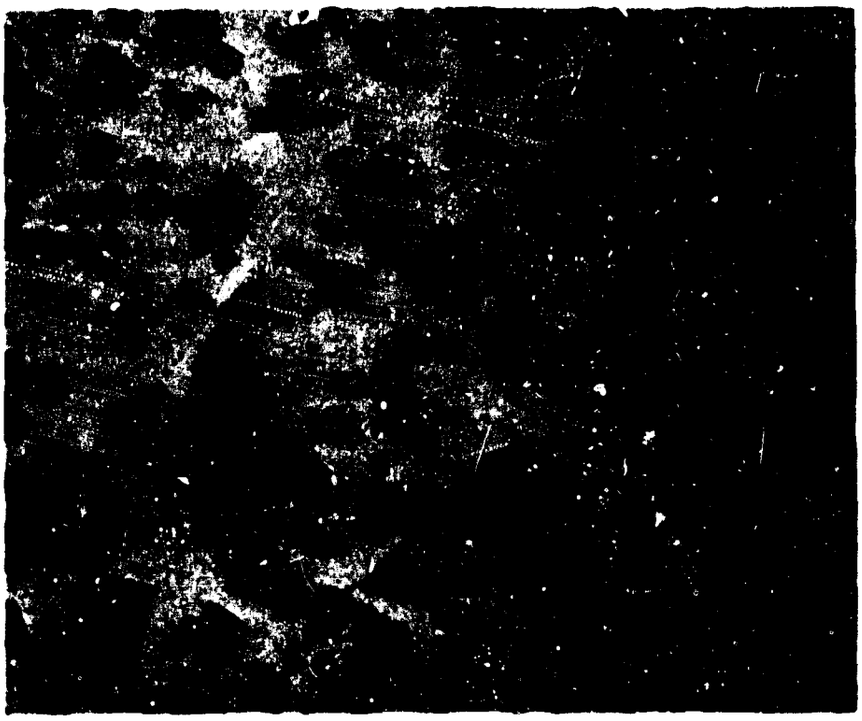

A. Ni + 75% TaC 300X

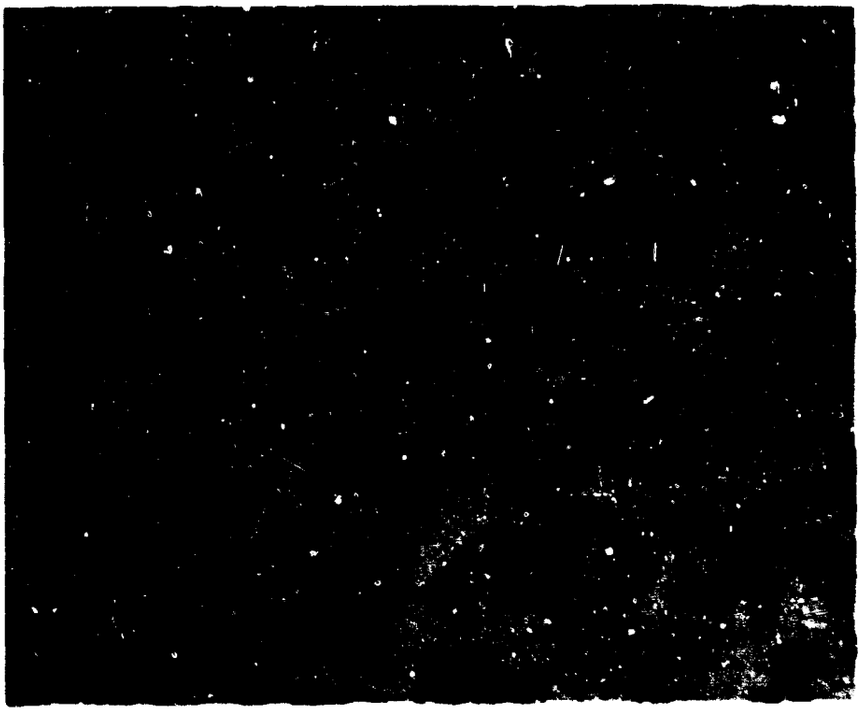

B. Ni + 100% TaC 600X

FIGURE D - 3 SOLUTION OF TaC IN NICKEL

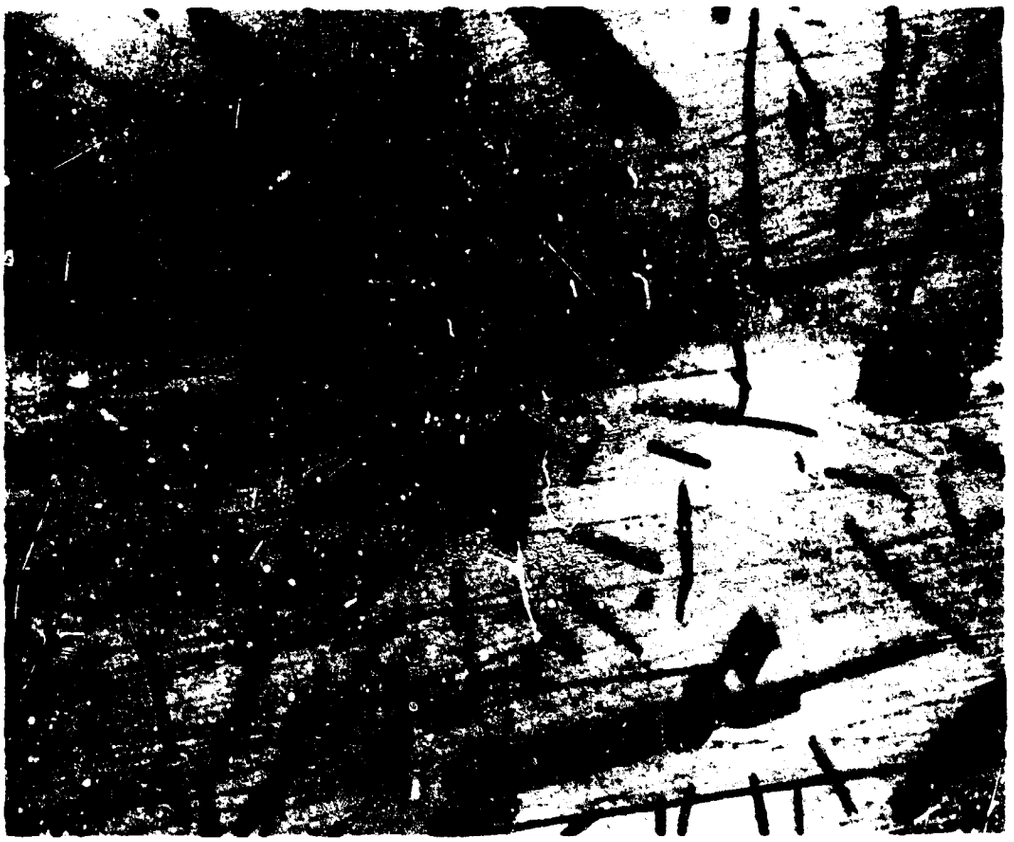

Ni + 20% TaC (melted in graphite crucible) 300X

FIGURE D - 4 SOLUTION OF TaC IN NICKEL

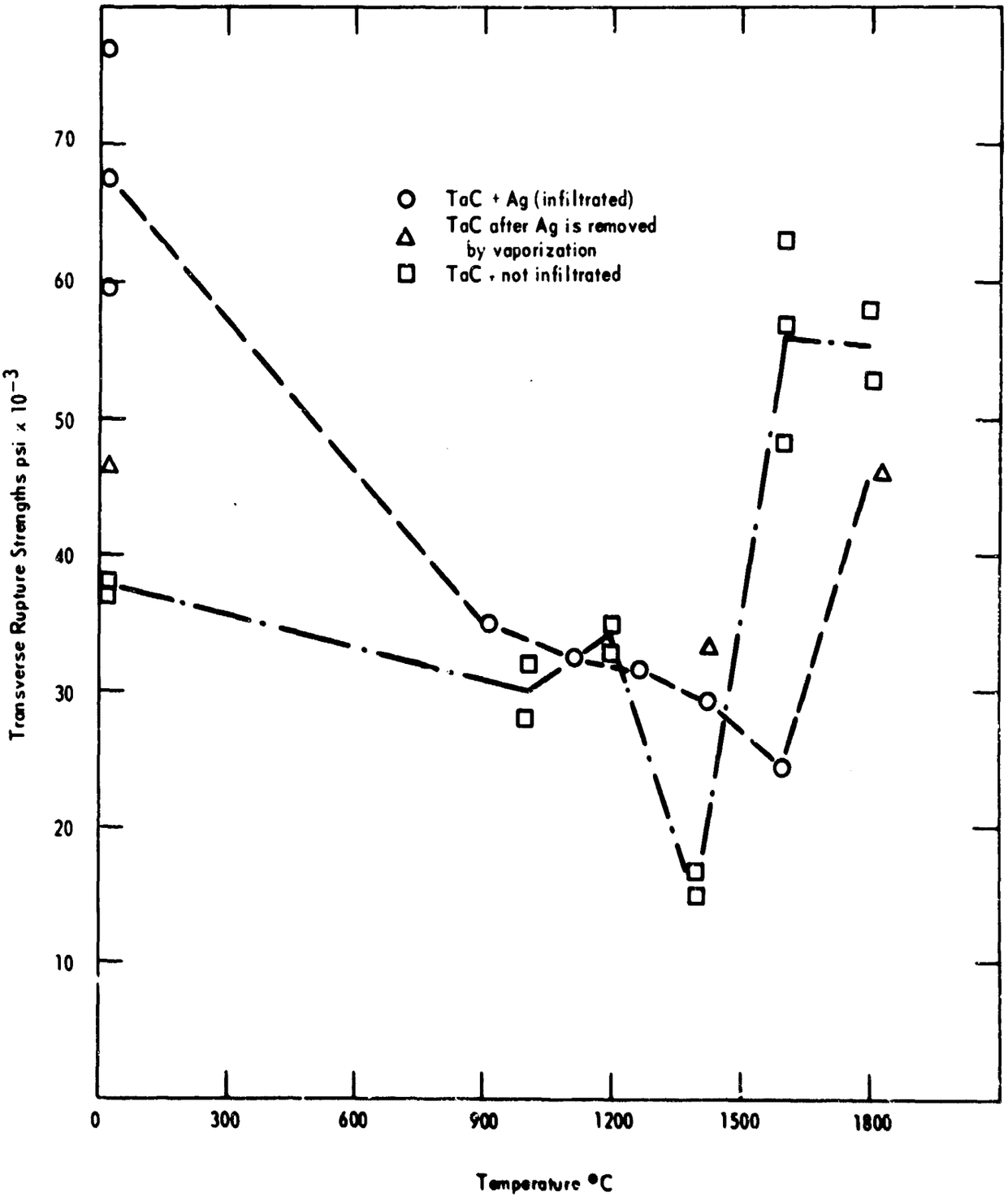

FIGURE D - 5 TRANSVERSE RUPTURE STRENGTHS VERSUS TEMPERATURE OF Ag INFILTRATED TaC

IV RECENT PUBLICATIONS AND PRESENTATIONS

Presentations

"Nozzle-Wall Chemical Corrosion", R. W. Kebler and R. A. Graff. Presented at the Nozzle Heat Transfer and Erosion Meeting sponsored by the Solid Rocket Division of the Air Force Rocket Propulsion Laboratory, Edwards Air Force Base, California, September 1, 1964.

"Kinetics of the Oxidation of Tungsten by CO_2 above 2000°K", I. R. Ladd, J. M. Quets, J. E. Smith, R. A. Graff, and P. N. Walsh. Presented at the Symposium on High-Temperature Chemistry of the Chemical Institute of Canada, September 2-4, 1964 in Ottawa, Ontario.

"Electrical Properties of Some Transition Metal Carbides and Nitrides", John Piper. Presented at the International Symposium on Compounds of Interest in Nuclear Reactor Technology, Boulder, Colorado, August 3-5, 1964.

Research Reports

"High Temperature Thermal Expansion of Certain Group IV and V Carbides", C. R. Houska, Research Report C-18, December 1963.

"The Reaction of Active Nitrogen with Graphite", H. W. Goldstein, Research Report C-19, December 1963.

"Bibliography on Analytical Chemistry Relating to Borides, Carbides, and Nitrides of Group IV and V Elements", M. R. Bateman, G. J. McKinley, G. H. Clewett, and H. F. Wendt, Research Report C-20, December 1963.

"Electrical Properties of Some Transition-Metal Carbides and Nitrides", John Piper, Research Report C-21, April 1964.

"Static Atomic Displacements Resulting From Vacancies in Defect Structures $TiN_x\square_{1-x}$", C. R. Houska, Research Report C-22, April 1964.

"Heat of Sublimation of Palladium", O. C. Trulson and P. O. Schissel, Research Report C-23, August 1964.

"Stagnation-Point-Velocity Distribution for a Compressible Fluid", R. A. Graff, Research Report C-24, October 1964.

"Mass Spectrometric Study of Zirconium Diboride", O. C. Trulson and H. W. Goldstein, Research Report C-25, October, 1964.

"Mass Spectrometric Study of the Oxidation of Tungsten", P. O. Schissel and O. C. Trulson, Research Report C-26, October 1964.

Publications

"The Reaction of Active Nitrogen With Graphite", H. W. Goldstein, J. Phys. Chem. 68, 39-42 (Jan. 1964).

"High-Temperature Furnace for Quantitative X-Ray Intensity Measurements", C. R. Houska and E. J. Keplin, J. Sci. Inst. 41, 23-27 (Jan. 1964).

"Thermal Expansion and Atomic Vibration Amplitudes for TiC, TiN, ZrC, ZrN, and Pure Tungsten", J. Phys. Chem. Solids 25, 359-366 (April 1964).

"Thermal Expansion of Certain Group IV and Group V Carbides at High Temperatures", C. R. Houska, J. Am. Cer. Soc. 47, 310-311 (June 1964).

"High-Temperature Ductility of Large-Grained TiC", F. G. Keihn and R. W. Kebler, J. Less Common Metals 6, 484 (June 1964).

"Electrical Properties of Some Transition Metal Carbides and Nitrides", John Piper, Nuclear Metallurgy (AIME) 10, 29 (August 1964).

V DISTRIBUTION

Advanced Research Projects Agency (5)
Washington 25, D. C.
Atn: Mr. T. O. Dobbins
Advanced Propellants Chemistry
Office

National Academy of Sciences
Washington, D. C.
Atn: Dr. Guy Waddington

National Aeronautics & Space Admin.
Washington 25, D. C.
Atn: Office of Technical Information
& Educational Programs CODE ETL

Atn: CODE MEG, Miss Carol Funk

Scientific & Technical Information
Facility (2)
Bethesda, Maryland
Atn: NASA Representative

National Aeronautics & Space Admin.
Lewis Research Center
Cleveland 35, Ohio
Atn: Library

National Aeronautics & Space Admin. (3)
Langley Research Center
Langley Air Force Base, Virginia
Atn: Library

National Aeronautics & Space Admin.
Goddard Space Flight Center
Greenbelt, Maryland
Atn: Library

National Aeronautics & Space Admin.
George C. Marshall Space Flight Center
Huntsville, Alabama
Atn: Library

National Aeronautics & Space Admin.
Manned Spacecraft Center
Houston 1, Texas
Atn: Library

National Bureau of Standards
Washington 25, D. C.
Atn: Dr. S. Madorskey

Atn: Dr. Charles W. Beckett, Jr.,
Chief (2)
Thermodynamic Section
Division of Heat & Power

Oregon Metallurgical Corporation
Albany, Oregon
Atn: Mr. Russell G. Hardy

U. S. Atomic Energy Commission
Office of Technical Information Ext.
Oak Ridge, Tennessee

U. S. Dept. of Interior
Bureau of Mines
Pittsburgh 13, Penn.
Atn: M M. Dolinar, Reports Lib.
Explosives Res. Laboratory

U. S. Bureau of Mines
Petroleum Research Center
Bartlesville, Oklahoma
Atn: Dr. John P. McCullough

Institute for Defense Analysis
400 Army-Navy Drive
Arlington, Va. 22202

U. S. Army Missile Command (5)
Redstone Arsenal, Alabama
Atn: Redstone Scientific Inf. Center

Atn: AMSMI-IXDA

Atn: AMSMI-RRP

Atn: AMSMI-IXD

Atn: AMSMI-RFE (8)

Atn: AMSMI-RK (Mr. R. J. Alley)

New York Procurement District
New York 3, New York
Atn: AMSMI-OBM

Chief, New York District
U. S. Army
New York 3, N. Y.
Atn: Facilities & Resources Branch

Atn: ORDEH-O-TA

Office, Chief of Ordnance
Washington 25, D. C.
Atn: ORDTB

Army Research Office
Duke Station
Durham, North Carolina

Atn: Dr. George Wyman, Box CM
Chemistry Division

Army Materials Research Agency
Watertown Arsenal
Watertown, 72, Mass.

Atn: Mr. A. P. Levitt, Chief
High Temperature Branch

Aberdeen Proving Ground, Maryland
Atn: Ballistic Research
Laboratory ORDBG-BLI

Picatinny Arsenal
Dover, New Jersey
Atn; Library

Diamond Ordnance Fuze Laboratories
Washington 25, D. C.
Atn: ORDTL (012)

U. S. Naval Air Missile Test Center
Point Mugu, California
Atn: Technical Library

U. S. Naval Ordnance Laboratory
White Oak, Silver Spring, Maryland
Atn: Library

U. S. Naval Ordnance Test Station
China Lake, California
Atn: Technical Library Branch

U. S. Naval Propellant Plant
Indian Head, Maryland
Atn: Technical Library

U. S. Naval Weapons Laboratory
Dahlgren, Virginia
Atn: Technical Library

Office of Naval Research
Washington 25, D. C.
Atn: CODE 429, Dr. Ralph Roberts

U. S. Naval Research Laboratory
Washington 20, D. C.
Atn: Chemistry Div. CODE 6130,
R. R. Miller

Bureau of Naval Weapons
Washington 25, D. C.
Atn: RMMP-2

Atn: RMMP-22, Mr. John J. Murrin

Atn: RMMP-3

Atn: RMMP-4

Atn: DLI-3 (2)

Atn: RRRE-6

Special Projects Office
Department of the Navy
Washington 25, D. C.

Aerojet-General Corporation (3)
Sacramento, California
Atn: Technical Information Office

Aerojet-General Corporation
Solid Rocket Plant, Bldg., 0525
Sacramento, Calif.
Atn: James P. Coughlin

Aerojet-General Corporation
Azusa, California
Atn: F. H. West, Chief Librarian

Aerojet-General Corporation
Structural Materials Div.
Azusa, Calif.
Atn: Dr. S. Brelant, Head
Materials Engineering Dept.

Aeronutronic, A. Div. of Philco Corp.
Newport Beach, Calif.
Atn: L. H. Linder, Manager
Technical Information Dept.

Atn: D. L. Hildenbrand

Aerospace Corporation (2)
Los Angeles 45, Calif.
Atn: Library - Documents

Air Force Flight Test Center
Edwards Air Force Base, California
Atn: FTR

Air Force Office of Scientific Research
Department of the Air Force
Washington 25, D. C.
Atn: Dr. Joseph Masi, Chief
Propulsion Div. (SREP)

AFML(MAMP/P.L. Faust)
Physical Metallurgy Branch
Metals and Ceramics Division
Wright-Patterson AFB, Ohio 45433

Air Force Systems Command (2)
Ceramics & Graphite Information Center
Wright-Patterson Air Force Base, Ohio
Atn: MAAM - (Mr. Barry R. Emrich)

Air Force Systems Command
Rocket Research Laboratories
Edwards, California
Atn: DGS

Atn: DGPS, Mr. Curtis C. Selph
Headquarters 6953d Test Group

Air Force Systems Command
Rocket Research Laboratory
Chemical & Materials Branch (DGPC)
Edwards, California 93523
Atn: Mr. Wayne C. Solomon

Air Force Systems Command (2)
Aeronautical Systems Division
Wright-Patterson Air Force Base, Ohio
Atn: Mr. W. G. Ramke, CODE ASRCMC

Atn: ASRCEM-1

Atn: ASRCNC-2

Atn: ASRCMP-2

Atn: ASRCTPT, Mr. Jules J. Wittebort

Air Force Systems Command
United States Air Force
AFSC Scientific & Techn. Liaison Office
New York 3, N. Y.

Air Force Unit Post Office
Space Systems Division
Los Angeles, Calif, 90045
Atn: SSSD

Air Proving Ground Center
Eglin Air Force Base, Florida
Atn: PGAPI

Air Research & Develop. Command
Headquarters, Wright Air Develop. Div.
Wright-Patterson Air Force Base, Ohio
Atn: WWRCPT-1

Air Research & Development Center
Andrews Air Force Base
Washington 25, D. C.
Atn: RDRAPR

Allied Chemical Corp.
General Chem. Division
Research Laboratory
Morristown, N. J.
Atn: L. J. Wiltrakis, Security Officer

Alpha Research & Development, Inc. (2)
Blue Island, Illinois
Atn: Dr. Robert Patrick

Amcel Propulsion Company
Asheville, North Carolina

American Cyanamid Company
Stamford, Conn.
Atn: Dr. Robert E. Torley

Atn: Dr. A. L. Pieker

Armour Research Foundation of Illinois
Institute of Technology
Chicago 16, Illinois
Atn: Fluid Dynamics & Propulsion
Research Dept. D.

Atn: Dr. Alan Snelson

Astro-Systems, Inc.
Caldwell, New Jersey
Atn: Mr. John S. Gordon

Atlantic Research Corporation
Shirley Highway & Edsall Road
Alexandria, Va.
Atn: Mr. Charles B. Henderson

Atomics International
Canoga Park, Calif.
Atn: S. C. Carniglia, Dept. 733

Battelle Memorial Institute
Columbus 1, Ohio
Atn: J. F. Lynch, Ceramics Div.

Atn: C. S. Dumont,
Defense Metals Info. Center

British Defense Staff (4)
British Embassy
Washington, D. C.
Atn: Scientific Information Center

The Carborundum Company
Niagara Falls, N. Y.

Chemical Propulsion Info. Agency
Applied Physics Laboratory
Silver Spring, Maryland
Atn: Mr. Gerald Avery

Clevite Corporation
Mechanical Research Division
Cleveland 8, Ohio
Atn: N. C. Beerli

Cornell Aeronautical Laboratories
Buffalo 21, New York
Atn: Mr. J. Beale

DeBell & Richardson, Inc.
Hazardville, Conn.
Atn: Mr. William Eakins

Defense Documentation Center (10)
Alexandria, Va.

Defense Research Member (4)
Canadian Joint Staff (W)
Washington 8, D. C.

The Dow Chemical Co. (2)
Midland, Michigan
Atn: Dr. Daniel R. Stull
Thermal Laboratory, Bldg. 574

Atn: Dr. R. S. Karpiuk
Security Section, Bldg., 1710

E. I. DuPont de Nemours & Co.
Eastern Laboratory
Gibbstown, N. J.
Atn: Mrs. Alice R. Steward

Esso Research & Engineering Co.
Chemicals Research Division
Special Projects Unit
Linden, N. J.
Atn: Dr. D. L. Baeder

Atn: Dr. Walter G. May

Fulmer Research Institute, Ltd.
Stoke Poges, Buckinghamshire, England
Atn: Dr. Philipp Gross

General Electric Company
Flight Propulsion Division
Evendale
Cincinnati, Ohio 45215

General Electric Co.
Nuclear Materials & Propulsion Oper.
Cincinnati, Ohio 45215
Atn: J. W. Stephenson

Hercules Powder Co. (2)
Allegany Ballistics Lab.
Cumberland, Maryland
Atn: Library

Hercules Powder Co.
Rocky Hill Plant
Rocky Hill, N. J.

Hercules Powder Co. (2)
Magna, Utah
Atn: Librarian

Ionics, Inc.
Washington 5, D. C.
Atn: Mr. S. G. McGriff,
Asst. Director of Research

Jet Propulsion Laboratory
Pasadena 3, Calif.
Atn: I. E. Newlan, Chief Reports Group.

Arthur D. Little, Inc.
Cambridge 40, Mass.
Atn: Dr. Alfred Buchler

Atn: Dr. J. B. Berkowitz-Mattuck

Lockheed Propulsion Co. (3)
Redlands, Calif.
Atn: Miss Belle Berlad, Librarian

Manufacturing Laboratories, Inc.
Cambridge 39, Mass.
Atn: Dr. Larry Kaufman

Midwest Research Institute
Kansas City 10, Mo.
Atn: Dr. Thomas A. Milne

Minnesota Mining & Manufacturing Co. (2)
St. Paul 6, Minnesota
Atn: CODE 0013 R&D
Via: H. C. Zeman
Security Administrator

Minnesota Mining & Manufacturing Co.
Central Research Laboratories
St. Paul 19, Minnesota
Atn: Dr. George Rathmann

National Research Corporation
Cambridge 42, Mass.
Atn: Mr. Ludwig Fasolino

Oak Ridge National Laboratory
Research Materials Information Center
Oak Ridge, Tennessee 37831

Olin Mathieson Chemical Corp. (2)
Research Library 1-K-3
New Haven, Conn.
Atn: Miss Laura M. Kajuti
Mail Control Room

Olin Mathieson Chemical Corp.
Marion, Illinois
Atn: Research Library

Rocketdyne (3)
Canoga Park, Calif.
Atn: Library 596-306

Atn: Mr. Kurt Mueller

Rocketdyne
A. Division of No. American Aviation, Inc.
Solid Propulsion Operations
McGregor, Texas
Atn: Library

Rocket Power
Pasadena, Calif.
Atn: Dr. Milton Farber, Vice Pres.

Shell Development Co.
Emeryville 8, Calif.

Space Technology Lab., Inc.
Redondo Beach, Calif.
Atn: Mr. Robert C. Anderson

Stanford Research Institute
Menlo Park, Calif.
Atn: G. M. Gordon

Thiokol Chemical Corporation
Redstone Division
Huntsville, Alabama
Atn: Technical Director

Thiokol Chemical Corporation
Elkton Division
Elkton, Maryland
Atn: Librarian

Thiokol Chemical Corporation
Reaction Motors Division
Denville, N. J.
Atn: Mr. William Mitchell

Thiokol Chemical Corp. (2)
Wasatch Div.
Brigham City, Utah
Atn: Library Section

Thiokol Chemical Corp.
Rockets Operation Center
Ogden, Utah
Atn: Librarian

United Aircraft Corporation
Research Laboratories
E. Hartford 8, Conn.
Atn: Mr. John D. Rockenfeller

United Technology Center
Sunnyvale, Calif.
Atn: Librarian

Atn: Dr. R. O. MacLaren

University of California
Los Alamos Scientific Lab.
Los Alamos, New Mexico 87544
Atn: Dr. James T. Waber

Dr. Leo Brewer
Department of Chemistry
University of California
Berkeley, California

Dr. S. H. Bauer
Department of Chemistry
Cornell University
Ithaca, New York

Professor R. L. Sproull
Materials Science Center
Cornell University, Thurston Hall
Ithaca, N. Y.

The John Hopkins University (3)
Solid Propellant Information Agency
Applied Physics Laboratory
Silver Spring, Maryland

The John Hopkins University
Applied Physics Laboratory
Silver Spring, Maryland
Atn: Dr. A. Westenberg

Dr. T. E. Phipps
Department of Chemistry
University of Illinois
Champaign-Urbana, Illinois

Dr. Charles J. Marsel
Department of Chemical Engineering
New York University
New York 53, N. Y.

Professor M. E. Fine
Materials Research Center
The Technological Institute
Northwestern University
Evanston, Illinois

Dr. Webster B. Kay
Dept. of Chemical Engineering
Ohio State University
Columbus 10, Ohio

Dr. David White
Department of Chemistry
Ohio State University
Columbus 10, Ohio

Dr. Robert D. Freeman
Department of Chemistry
Oklahoma State University
Stillwater, Oklahoma

Professor J. N. Hobstetter
Laboratory for Res. on Struc. of Matter
University of Pennsylvania
Philadelphia 4, Penna.

Dr. Y. S. Touloukian
Dir., Thermophysical Prop. Res. Cen.
Purdue University
West Lafayette, Indiana

Professor J. L. Margrave
Department of Chemistry
Rice Institute
Houston 11, Texas

Dr. K. Keith Innes
Department of Chemistry
Vanderbilt University
Nashville, Tennessee

Professor Paul R. Jones
Dept. of Chemical Engineering
West Virginia University
Morgantown, West Va.

Dr. Paul Bender
Department of Chemistry
University of Wisconsin
Madison, Wisconsin

Dr. Peter McCuen
Vidya Company
Stanford Industrial Park
Palo Alto, Calif.

Westinghouse Electric Co.
Pittsburgh, Penn.
Atn: Dr. Alvin Boltax

Wright Aeronautical Div.
Curtiss-Wright Corp.
Woodridge, N. J.

Union Carbide Corporation

Dr. A. L. Bayes

Mr. J. C. Bowman

Dr. J. C. Brantley/ G. H. Clewett/
UCN Library

Dr. R. M. Bushong

Mr. M. C. Carosella

Dr. R. A. Charpie

Mr. M. E. Cieslicki

Mr. D. E. Hamby

Dr. A. B. Kinzel

Helen F. Kuhns, Librarian
Union Carbide Stellite Div.

Dr. P. Lafayatis

Dr. M. A. Lynch

Mr. W. Manly

Dr. R. W. McNamee

Mr. R. M. Milton

Dr. W. J. Spry

Dr. Milton Stern

Mr. W. A. Steiner

Mr. D. Swan

Mr. H. F. Wendt/
Mr. A. L. Hallowell

Mr. H. L. Willard

Dr. C. E. Winters